UNIVERSITA' DEGLI STUDI DI PADOVA

DIPARTIMENTO DI SCIENZE DEL FARMACO

CORSO DI DOTTORATO DI RICERCA IN SCIENZE FARMACOLOGICHE

Curricolo: Farmacologia Cellulare e Molecolare

Ciclo: XXIX

Generation and characterization of a new model of OPA1- linked Dominant Optic Atrophy

Coordinatore: Ch.mo Prof. Piero Maestrelli

Supervisore: Dott.ssa Monica Montopoli

Co-Supervisore: Dott. Andrea Daga

Dottorando: Aldo Montagna

INDEX

Summary

Mitochondria are very dynamic organelles with a crucial role in life and death of eukaryotic cells. These organelles regulate cellular energy generation, calcium and redox homeostasis, and apoptosis. To perform the cellular functions effectively, mitochondria continuously change their structure and morphology through protein machineries controlling fission and fusion process (mitochondrial dynamics). Strong evidence has emerged to implicate disturbed mitochondrial fusion and fission as central pathological components underpinning a number of childhood and adult-onset neurodegenerative disorders. Several proteins that regulate the morphology of the mitochondrial network have been identified, the most widely studied of which are Optic Atrophy 1 (OPA1), Mitofusin1 and 2 (Mfn1 and 2) and Dynamin Related Protein 1 (DRP1).

OPA1 is a ubiquitously expressed dynamin-like GTPase in the inner mitochondrial membrane. It plays important roles in mitochondrial fusion, apoptosis, reactive oxygen species (ROS) and ATP production. Mutations of OPA1 result in autosomal Dominant Optic Atrophy (DOA), a common hereditary optic neuropathy characterized by retinal ganglion cell degeneration leading to optic neuropathy, symmetrical central visual loss and dyschromatopsia. The majority of OPA1 mutations result in premature termination codons, and the resultant truncated mRNA species are highly unstable, being rapidly degraded by protective surveillance mechanisms operating via nonsense-mediated mRNA decay. Haploinsufficiency, therefore, is a major disease mechanism in DOA, and the pathological consequences of a dramatic reduction in OPA1 protein levels is highlighted by those rare families who are heterozygous for microdeletions spanning the entire OPA1 coding region. Progressive visual failure remains the defining feature of DOA but, with greater availability of genetic testing, a specific OPA1 mutation in exon 14 (c.1334G>A, p.Arg445His) has been found to cause sensorineural deafness, ataxia, myopathy, peripheral neuropathy, and classical chronic progressive external ophthalmoplegia. This syndrome is called DOA plus.

The molecular mechanisms linking OPA1 mutations and DOA are not fully understood. In this work a new model of OPA1-linked Dominant Optic Atrophy was generated in *Drosophila melanogaster,* in order to use it for studying DOA pathogenesis.

The *Drosophila* OPA1 gene (*dOPA1*) shares 51.2% similarity with its human orthologue and the alignment of protein sequence of *hOPA1* with *dOPA1* shows that the domains most subjected to pathogenic mutations are well conserved.

To address the pathophysiological mechanism of OPA1-linked DOA, we generated two *dOPA1* mutants: OPA1 *R417H*, a mutant that carries in endogenous dOPA1 the mutation corresponding to R445H in humans; OPA1^{null} carrying a microdeletion leading to production of a inactive truncated protein of 482 amino acids.

To model these mutations we have used in vivo CRISPR/Cas9, a genome engineering system that has revolutionized genetic analysis in many organisms. For use in genome engineering the system requires two essential components: gRNA and Cas9-endonuclease. The gRNA recognizes a 20-nt target sequence next to a trinucleotide NGG protospacer adjacent motif (PAM) to direct Cas9-dependent cleavage of both DNA strands within the target sequence. Several groups have used the CRISPR/Cas9 system to induce targeted mutations in *Drosophila,* but differ in their approach to supply the Cas9 protein and gRNA components of the system. It has been demonstrated that two targeting gRNAs can be used to generated a large defined deletions and the Cas9 catalyzed gene replacement by homologous recombination.

The experimental design of my work requires the following steps: generation of the gRNAs responsible for precisely targeting the genomic region where recombination should take place; generation of the dsDNA templates containing the desired genomic modifications to be introduced and homology arms for accurate recombination; choice of a screening method.

The gRNAs guide the cut of the Cas9 on the genomic region of the dOPA1 gene through the target sequences and the PAM sites; the cut of genomic DNA favors homologous recombination with the dOPA1 mutated fragment cloned into dsDNA plasmid donor. The exogenous dOPA1 mutated gene in addition to the pathological mutations carries a silent mutation that introduces a novel

BamHI restriction site necessary for screening the occurrence of homologous recombination events by restriction digest.

The gRNAs and the dsDNA plasmids donors were microinjected in the embryo of the *Drosophila* line expressing Cas9 protein in the ovary under control of *vasa* regulatory sequences.

The mutants were screened for the presence of the mutation through PCR on genomic DNA, restriction digest and sequencing of the OPA1 mutated fragment. After having verified that the mutants had mutations of interest without any other alterations, we described the phenotypic effects observed in these mutants. We also analyzed the mitochondria in the nervous and muscular systems using confocal microscopy and the mitochondrial functions through biochemical assays.

Observations of the adults within the lines shows that both mutations in heterozygosity do not cause any evident morphological alterations. However, both mutations in homozygosity turned out to be lethal but differently R417H homozygous mutants develop until the second instar larva stage whereas the OPA1^{null} homozygotes die earlier at the first instar larva stage.

We were more interested in studying the heterozygote *dOPA1* mutants because DOA is a dominant disease. The lifespan reduction of both *dOPA1* mutants indicate that the heterozygous mutations of OPA1 is likely to cause systemic consequences probably affecting multiple processes. Since OPA1 is involved in mitochondrial dynamics we performed a series of experiments to analyze mitochondrial morphology in the neuronal and muscular systems of both *dOPA1* mutants. Heterozygous dOPA1 mutants display defects of mitochondria morphology in nerves and muscles in *Drosophila* third instar larvae, mitochondria network shape is characterized by mild fragmentation and clusterization. Mitochondria function was analyzed on homozygous and heterozygous dOPA1 mutants. Mitochondrial respiration and the redox activity of respiratory complexes was decreased in both mutants. Furthermore heterozygous OPA1 R417H displayed more severe effects in some assays than OPA1null heterozygotes. This suggested that R417H mutation could interfere with the activity of the wild type copy of *dOPA1* resulting in more severe phenotypes than those caused by the presence of a single loss of function allele.

In conclusion, we have produced a model to study the Dominant Optic Atrophy which can be helpful to understand the pathogenesis of this disease caused by different classes of mutations within the OPA1 gene.

Riassunto

I mitocondri sono organelli dinamici fondamentali per la vita e la morte delle cellule eucariotiche, svolgono diverse funzioni tra cui: produzione di ATP, regolazione dell'omeostasi del Ca^{2+}, produzione di ROS e regolazione dell'apoptosi. I processi di fusione e fissione mitocondriale (dinamiche mitocondriali) sono alla base del corretto funzionamento di questi organelli e sono controllati da una serie di proteine che, di conseguenza, regolano forma e struttura dei mitocondri.

Disturbi delle dinamiche mitocondriali sono alla base di diverse patologie neurodegenerative che colpiscono bambini e giovani adulti. Le diverse proteine che regolano la morfologia della network mitocondriale sono state individuate in vari studi, le principali sono: Optic Atrophy 1 (OPA1), Mitofusin1 and 2 (Mfn1 and 2) and Dynamin Related Protein 1 (DRP1).

OPA1 è una proteina ubiquitaria della famiglia delle dianamine, con attività GTPasica, situata sulla membrana interna dei mitocondri. Presenta un ruolo fondamentale nel processo di fusione mitocondriale, apoptosi, produzione di ROS e produzione di ATP. Mutazioni di OPA1 sono alla base dell' Atrofia Ottica Dominante (DOA), una comune neuropatia ottica ereditaria caratterizzata da degenerazione delle cellule ganglionari della retina con conseguente neuropatia, perdita della capacità visiva simmetrica centrale e discromatopsia. La maggior parte delle mutazioni patologiche di OPA1 determinano la formazione di codoni di stop, con conseguente produzione di forme troncate di mRNA altamente instabili che vengono rapidamente degradate dai vari meccanismi di controllo. L'aploinsufficienza è il principale meccanismo patogenetico della DOA, le conseguenze di una drastica riduzione dei livelli di OPA1 sono ben visibili in famiglie in cui sono state identificate microdelezioni in eterozigosi, localizzate nella regione codificante del gene di OPA1. La perdita progressiva della vista rimane la caratteristica principale della DOA ma, la maggior disponibilità di test genetici, ha permesso di identificare una mutazione specifica del gene OPA1 localizzata sull'esone 14 (c.1334G>A, p.Arg445His) che causa DOA, associa a sordità neurosensoriale, atassia, miopatia, neuropatia periferica e oftalmoplegia esterna progressiva cronica. Questa sindrome è chiamata DOA plus.

I meccanismi molecolari alla base di DOA causata da mutazioni di OPA1 non sono del tutto chiari. In questo lavoro abbiamo generato un nuovo modello di Atrofia Ottica Dominante usando *Drosophila melanogaster*, al fine di utilizzarlo per studiare e comprendere al meglio la patogenesi di questa malattia.

Il gene OPA1 di *Drosophila* (*dOPA1*) mostra il 51.2% di similarità con il gene ortologo umano, l'allineamento della proteina umana con quella di *Drosophila* mostra che i domini, su cui si localizzano la maggior parte delle mutazioni patologiche, sono altamente conservati.

Per studiare il meccanismo patofisiologico della DOA dovuta a mutazioni di OPA1, abbiamo generato due mutanti *dOPA1*: OPA1 R417H, un mutante che porta la mutazione corrispondente alla mutazione umana OPA1 R445H; e il mutante OPA1^{null} in cui è stata inserita una microdelezione che determina la produzione di una forma tronca inattiva di 482 aminoacidi.

Per inserire queste mutazione nel genoma di *Drosophila* abbiamo utilizzato il sistema CRISPR/Cas9, un sistema che permette la modifica del DNA genomico e che ha rivoluzionato le analisi genetiche in diversi organismi. Le componenti fondamentali di questo sistema sono gRNA e endonucleasi Cas9. Il gRNA riconosce una sequenza target di 20nt seguita da un sito PAM (protospacer adjacent motif), costituito da tre nucleotidi NGG, e necessario per indirizzare il taglio dei due filamenti del DNA genomico ad opera dell'endonucleasi Cas9. Diversi gruppi di ricercatori hanno utilizzato il sistema CRISPR/Cas9 per introdurre specifiche mutazioni nel genoma di *Drosophila*, mettendo a punto vari metodi di somministrazione delle diverse componenti. È stato dimostrato che un approccio metodologico efficace, è l'utilizzo di una coppia di gRNA che, mediante il taglio del Ca9, determinano una larga delezione in una porzione genomica ben definita e questo, in presenza di una dsDNA donatore, favorisce la sostituzione genica mediante ricombinazione omologa.

Il disegno sperimentale del mio lavoro richiede i seguenti steps: generazione dei gRNA in grado di indirizzare il taglio dell'endonucleasi sulla regione genomica di interesse; generazione del dsDNA donatore contenete la porzione genica con le mutazioni desiderate e due regioni di omologia limitrofe ad essa e necessarie per la corretta ricombinazione e infine la scelta di un metodo di screening.

I gRNA guidano il taglio del Cas9 sulla porzione genomica del gene dOPA1 grazie alla sequenza target di 20nt e ai siti PAM; il taglio del DNA genomico favorisce la ricombinazione omologa con il frammento mutato di dOPA1 clonato nel plasmide dsDNA donatore. Sul frammento genico esogeno, oltre alla mutazione patologica di OPA1, è stata inserita una mutazione silente per introdurre un sito di restrizione dell'enzima BamHI, necessario per lo screening dei mutanti in cui è avvenuta la corretta ricombinazione.

I gRNAs e i plasmidi dsDNA donatori sono stati microiniettati in embrioni di una linea di *Drosophila* in cui la proteina Cas9 è espressa nelle cellule germinali, sotto il controllo del fattore di regolazione della trascrizione genica, *vasa.*

Lo screening per individuare i mutanti corretti è stato fatto mediante PCR sul DNA genomico, taglio di restrizione e sequenziamento. Dopo aver verificato la corretta ricombinazione omologa del frammento esogeno abbiamo eseguito una caratterizzazione fenotipica dei mutanti. Mediante microscopia confocale, abbiamo analizzato la morfologia dei mitocondri nel sistema nervoso e muscolare; con dei saggi biochimici abbiamo poi testato la funzionalità mitocondriale in larve mutanti.

Gli adulti eterozigoti per le mutazioni di dOPA1 non presentano evidenti alterazioni morfologiche. Entrambe le mutazioni però, risultano letali in omozigosi ma con delle differenze: la mutazione R417H risulta essere letale al secondo stadio larvale mentre la completa assenza di OPA1, che si determina nel mutante omozigote OPA1^{null}, è letale al primo stadio larvale. Essendo DOA una malattia genetica dominante, è importante studiare gli effetti di queste mutazioni sui mutanti eterozigoti. Analizzando la durata media della vita dei mutanti adulti eterozigoti, abbiamo osservato un importante riduzione di questo parametro, simile per entrambe le mutazioni e collegato probabilmente agli effetti sistemici che si hanno in seguito all'alterazione di vari processi cellulari che coinvolgono OPA1 e i mitocondri. Dato che OPA1 è una proteina coinvolta nella regolazione delle dinamiche mitocondriali, abbiamo messo a punto una serie di esperimenti per analizzare la morfologia mitocondriale nel sistema nervoso e muscolare dei mutanti dOPA1. In larve terzo stadio eterozigoti per entrambe le mutazioni abbiamo osservato alterazioni della morfologia mitocondriale in nervi e muscoli, il network mitocondriale è caratterizzato da lieve frammentazione e presenza di cluster. La funzionalità mitocondriale è

stata analizzata nei mutanti dOPA1 eterozigoti ed omozigoti. Respirazione mitocondriale e attività redox dei complessi della catena respiratoria risultano ridotte in entrambi i mutanti. Inoltre, il mutante OPA1 R417H eterozigote risulta avere deficit di funzionalità mitocondriale maggiore rispetto al mutante OPA1^{null} eterozigote. Questo suggerisce che la mutazione R417H possa interferire con l'attività della copia wild type di *dOPA1,* determinando un fenotipo più grave della perdita di un solo allele funzionante.

Per concludere, possiamo affermare di aver prodotto un modello di Atrofia Ottica Dominate che potrebbe essere d'aiuto per lo studio della patogenesi di questa malattia e per comprendere meglio come agiscono le diverse classi di mutazioni sul gene OPA1.

1.INTRODUCTION

Mitochondria are fundamental organelles in life and death of eukaryotic cells. They are the main site of energy production and they have a central position in the programmed cell death pathway. Moreover, they are involved in many others processes, such as Ca^{2+} homeostasis, cellular differentiation, control of cell cycle and growth, amplification of signaling cascades. Finally, mitochondria are involved in several human diseases, including neurodegenerative disorders and cancer, and may play a role in aging processes.

The structure of these organelles is very elaborate and supports their multiple functions. In certain cell types they are organized in networks of interconnected mitochondria. Similarly, the ultrastructure of mitochondria is extremely complex, with the organelle bound by two distinct membrane: the outer membrane (OMM) and the inner membrane (IMM).

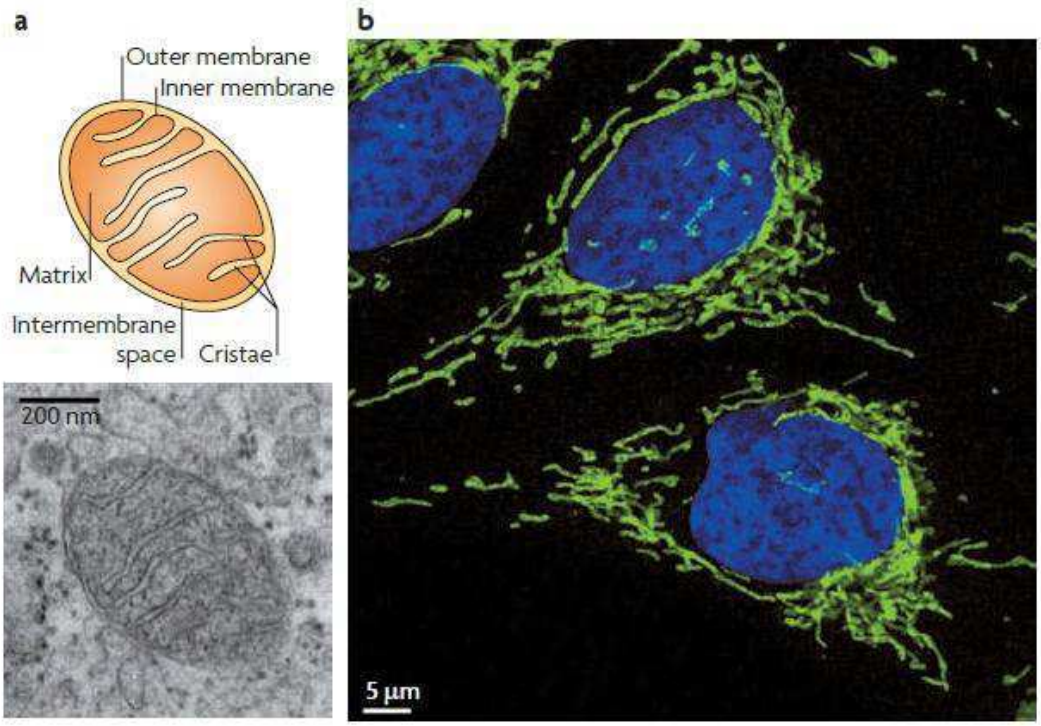

Figure 1: Mitochondrial morphology. **(A)** Mitochondria are double membrane-bound organelles with characteristic inner membrane folds, termed cristae. The schematic shows the structure of mitochondria. A transmission electron microscopy image of mitochondria in ultrathin sections of human fibroblast cells is also shown. **(B)** In many cell types, mitochondria appear as long, tubular and sometimes branched structures that spread throughout the entire cytoplasm. Mitochondria (green) were stained in human osteosarcoma cells (U2OS) by indirect immunofluorescence using antibodies against the outer membrane protein TOM20.Nuclei (blue) were stained with DAPI (4′,6-diamidino-2-phenylindole). Cells were analysed by confocal microscopy.[1]

The IMM is organized in distinct compartments, the peripheral inner membrane and the *cristae* that are separated from the peripheral inner membrane by narrow tubular junction (Figure 1a). The cristae are key mitochondrial structures: they are the site of oxidative phosphorylation where the complexes of respiratory chain are localized. Furthermore live cell microscopy studies showed that mitochondria are highly dynamic organelles that can build large interconnected intracellular networks (Figure 1b). In many eukaryotic cell types, mitochondria continuously move along cytoskeletal tracks and frequently fuse and divide. These concerted activities control mitochondrial morphology and intracellular distribution and determine their cell type-specific appearance[1].

The morphology of the mitochondrial network is in a constant state of flux, influenced by the delicate balance between opposing fusional and fissional forces. The main players in this intricate and tightly coordinated process were first identified in seminal experiments using yeast models. These mediators of mitochondrial dynamics have been highly conserved throughout evolution, which is in keeping with the critical regulatory roles of these proteins in both simple and complex organisms. Pathogenic mutations have been identified in several pro-fusion and pro-fission nuclear genes, with disease phenotypes ranging from severe, early-onset and invariably lethal encephalomyopathies, through isolated optic atrophy and peripheral neuropathy, to more-complex late-onset multisystemic neuromuscular disorders. Mutations in the pro-fusion genes optic atrophy 1 (OPA1) were initially reported in families with autosomal dominant optic atrophy (DOA; OMIM #605290)[2].

1.1 Mitochondrial network dynamics

Research on mitochondrial fusion and fission (collectively termed mitochondrial dynamics) gained much attention in recent years, as it is important for our understanding of many biological processes, including the maintenance of mitochondrial functions, apoptosis and ageing.

Mitochondria in cells of most tissues are tubular, but dynamic changes in morphology are driven by fission, fusion and translocation (Figure 2)[3].

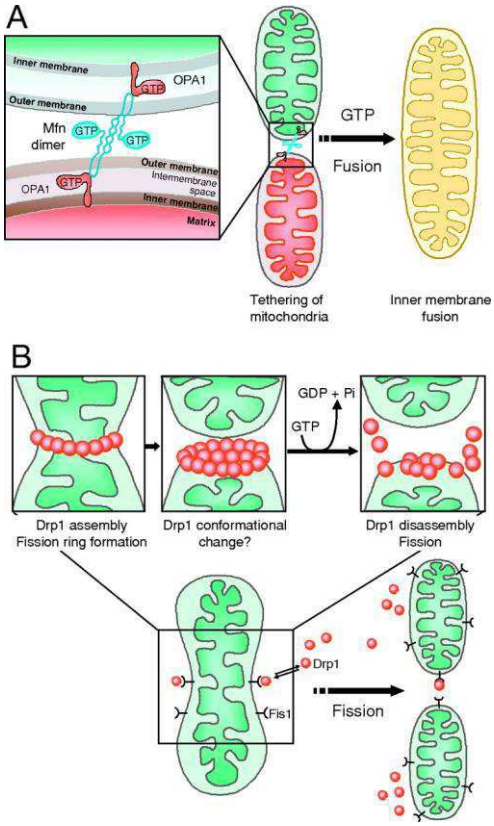

Figure 2: Mitochondrial fusion and fission dissected. **(A)** Fusion of mitochondria requires the sequential interaction of outer and inner membranes. Fusion of the outer membranes of two adjacent mitochondria requires low GTP levels, whereas the subsequent fusion of the inner membranes requires high GTP levels. Two components of the mitochondrial fusion machinery are known in mammalian cells, the outer membrane proteins mitofusins Mfn1 and Mfn2, which each have a cytosolic GTPase domain and two coiled-coil regions, and the intermembrane space proteins GTPase OPA1. **(B)** Models and molecules of mitochondrial fission. Fission protein 1 (Fis1) is localized uniformly to the mitochondrial outer membrane, whereas dynamin-related protein (Drp1) is localized to the cytosol and punctate spots on mitochondria. Some of these spots are constriction sites that lead to mitochondrial fission. How Drp1 is recruited to mitochondria is unclear.

Mechanisms of mitochondrial fusion

Membrane fusion is a fundamental process in the life of eukaryotic cells. For example, transport vesicles fuse with the organelles of the secretory pathway,

gametes fuse during fertilization, and enveloped viruses enter the host cytosol by fusion with endosomal membranes. Mitochondrial fusion is a particularly complex process, as mitochondria are double membrane-bound organelles and must coordinate the fusion of four membranes.

The first known mediator of mitochondrial fusion was identified in 1997 by molecular genetic analysis of the male sterile fuzzy onions (fzo) mutant in Drosophila melanogaster[4]. Mitofusins in yeast and metazoa share a similar domain structure. They are large GTPases that contain two transmembrane regions in the mitochondrial outer membrane, with a short loop in the intermembrane space and the major parts of the protein facing the cytosol[5,6].

Yeast Fzo1 contains three predicted heptad repeat regions. Mammals have two mitofusin isoforms, MFN1 and MFN2, both of which lack the most amino-terminal heptad repeat.

Mgm1 is a dynamin-related large GTPase that is essential for inner membrane fusion in yeast[7]. It has an N-terminal mitochondrial targeting sequence that is cleaved by matrix-processing peptidase (MPP) following import. A large Mgm1 isoform contains an N-terminal transmembrane domain that anchors the protein in the inner membrane, and its main part is located in the intermembrane space. A fraction of Mgm1 molecules is processed further during import by the rhomboid-related membrane protease Pcp1, generating a short isoform that lacks the transmembrane anchor[8]. Both isoforms contain a GTPase domain, a GTPase effector domain and several heptad repeats. The mammalian Mgm1 orthologue, optic atrophy protein 1 (OPA1), and related proteins in worms and flies have also been shown to be required for mitochondrial fusion[9,10]. OPA1 is present in eight isoforms that are generated by alternative splicing and alternative processing at two cleavage sites that are located between the N-terminal transmembrane domain and the first heptad repeat.

During fusion two mitochondria approaching each other are tethered in a docking step, consistently the carboxy-terminal heptad repeats of mammalian MFN1 have been shown to form an intermolecular antiparallel coiled coil that may tether adjacent mitochondria prior to fusion[11]. Coiled coil formation by mitofusins might then draw the membranes close together and initiate lipid bilayer mixing, and the GTPase could provide biomechanical energy for outer membrane fusion.

The first mechanistic insights into the role of Mgm1 in inner membrane fusion came from the analysis of yeast mutant mitochondria in vitro. After the completion of outer membrane fusion, Mgm1 is required in trans on both inner membranes of the fusion partners. Certain *mgm1* mutant alleles show a specific defect in inner membrane tethering, whereas others are defective in inner membrane fusion, suggesting that Mgm1 participates in both processes[7]. Interestingly, studies using purified Mgm1 variants reconstituted with liposomes showed that only the short Mgm1 isoform, which lacks the transmembrane region, has GTPase activity, and that its GTPase is activated in heterotypic complexes containing the membrane-bound long isoform. Thus, the long Mgm1 isoform is proposed to tether opposing inner membranes and harness GTPase dependent conformational changes of the short isoform to initiate lipid bilayer mixing of the inner membrane[12].

Mechanisms of the mitochondrial fission

Dynamin superfamily members are versatile large GTPases that mediate various membrane remodeling processes in eukaryotic cells. Mgm1 and OPA1, and in particular Fzo1 and mitofusins, are distantly related dynamin superfamily members. Although these proteins function in membrane fusion, classical dynamins are typically involved in membrane scission events in vesicle budding pathways. Classical dynamins assemble into higher oligomeric structures that form rings and spirals around membranes. These spirals are thought to sever the enclosed membranes following GTP hydrolysis through the mechanoenzymatic activity of dynamin[1]. Dynamin-related proteins have similar roles in the division of membrane-bound organelles, including endosomes, peroxisomes and mitochondria.

A dynamin-related protein, termed Dnm1 in yeast and dynamin-related protein 1 (DRP1) in mammals, is the master regulator of mitochondrial division in most eukaryotic organisms. It is a soluble protein containing an N-terminal GTPase, a middle domain and a C-terminal GTPase effector domain that is involved in self-assembly. Cells lacking DRP1 contain highly interconnected mitochondrial nets that are formed by ongoing fusion in the absence of fission activity[13].

The function of the mitochondrial fission machinery is best understood in yeast. Recruitment of Dnm1 from the cytosol and assembly in punctate structures on the mitochondrial surface depends on two partner proteins, mitochondrial

fission-1 (Fis1) and mitochondrial division protein 1 (Mdv1)[14]. Fis1 is a small tailanchored protein in the outer membrane. Its N-terminal domain faces the cytosol, where it forms a six-helix bundle with tandem *tetratricopeptide repeat motifs* (TPR) that provide an interface for interaction with the adaptor protein Mdv1[15]. Mdv1 contains an N-terminal extension for Fis1 binding, a heptad repeat region mediating homo-oligomeric interactions and a C-terminal WD40 repeat domain that interacts with Dnm1[16].

Recent *in vitro* studies using purified proteins revealed mechanistic insights into the role of Mdv1 as a dynamin effector that mediates the assembly of Dnm1 and suggests the following model of mitochondrial division in yeast. First, Fis1 recruits Mdv1 from the cytosol. Membrane-associated Mdv1 then nucleates the assembly of Dnm1–GTP oligomers on the mitochondrial surface. Dnm1–GTP oligomers proceed to form spirals that are eventually wrapped around the organelle. Finally, Dnm1 spirals sever the mitochondrial membranes following GTP hydrolysis in a manner that is probably similar to the action of classical dynamins in vesicular budding pathways[17,18].

In mammals FIS1 interacts with DRP1 and apparently has a similar role in mitochondrial fission to its yeast counterpart, as FIS1 overexpression promotes mitochondrial fragmentation and FIS1 depletion produces interconnected mitochondrial nets[19, 20]. However, Mdv1 homologues have not been identified in metazoans which indicates significant differences between the metazoan and yeast mitochondrial division machineries. Furthermore, knockdown of human FIS1 does not affect the distribution of DRP1 in mitochondria[21], and deletion of the two FIS1 homologous genes in *Caenorhabditis elegans* does not produce a strong mitochondrial fission phenotype[22], suggesting that additional pathways of DRP1 recruitment exist in metazoans. One possible candidate for an alternative fission factor is mitochondrial fission factor (MFF), a tail-anchored protein that is conserved in metazoans but does not exist in yeast. MFF contains heptad repeats and a C-terminal transmembrane domain that is embedded in the outer membrane. Depletion of MFF attenuates mitochondrial division, both in mammalian and *D. melanogaster* cells. Interestingly, MFF and FIS1 exist in separate complexes, suggesting that they have different roles in mitochondrial division[23].

Functions of mitochondrial dynamics

Mitochondria cannot be generated *de novo*; instead, they proliferate by growth and division of pre-existing organelles. They contain their own genome and protein translation machinery. mtDNA is present in multiple copies and packed into compact particles, termed *nucleoids*. It encodes ribosomal RNAs, tRNAs and some proteins required for respiration. However, most mitochondrial proteins are encoded by nuclear genes and synthesized by cytosolic ribosomes. Mitochondrial biogenesis involves the import of nucleus-encoded proteins from the cytosol, the incorporation of mitochondrion synthesized and imported membrane lipids, the amplification of the mitochondrial genome and the translation of mitochondrion-encoded proteins. Damaged and surplus organelles are removed by autophagy. During their life cycle, mitochondria fuse with each other and split apart again; fusion serves to mix and unify the mitochondrial compartment, whereas fission generates morphologically and functionally distinct organelles. These processes have important consequences for mitochondrial functions in cell life and death (Figure 3)[1].

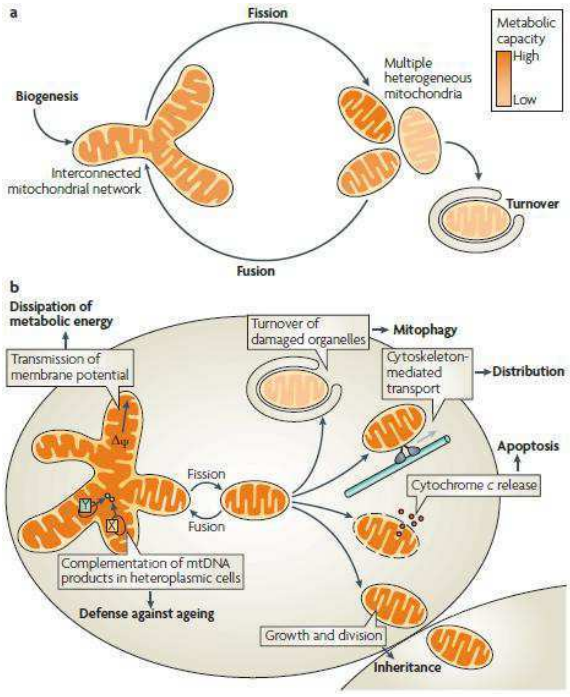

Figure 3: Biological functions of mitochondrial dynamics. **(A)** The mitochondrial life cycle starts with growth and division of pre-existing organelles (biogenesis) and ends with degradation of impaired or surplus organelles by mitophagy (turnover). In between, mitochondria undergo frequent cycles of fusion and fission that allow the cell to generate multiple heterogeneous mitochondria or interconnected mitochondrial networks, depending on the physiological conditions. **(B)** Fusion and fission of mitochondria are important for many biological functions. Division is required for inheritance and partitioning of organelles during cell division, for the release of pro-apoptotic factors from the intermembrane space, for intracellular distribution by cytoskeleton-mediated transport and for turnover of damaged organelles by mitophagy. Fused mitochondrial networks are important for the dissipation of metabolic energy through transmission of membrane potential along mitochondrial filaments and for the complementation of mitochondrial DNA (mtDNA) gene products in heteroplasmic cells to counteract decline of respiratory functions in ageing (X and Y depict alleles of different mitochondrial genes).[1]

Mitochondrial dynamics is essential in mammalian development. Mitochondrial fusion is important for inheritance and maintenance of mtDNA. In yeast, fusion-defective mutants rapidly lose their mitochondrial genome and consequently show defects in respiration[24]. This is probably because fragmentation of mitochondria produces multiple small organelles, most of which lack mtDNA, so partitioning of these organelles to daughter cells produces a significant number of progeny lacking mtDNA. As a result, mitochondrial genomes are lost from the population after several generations.

Disruption of fusion in mammalian cells also leads to mitochondrial heterogeneity and dysfunction, possibly as a consequence of nucleoid loss in individual mitochondria[25]. Thus, it seems that fusion serves as a fundamental mechanism to maintain a mitochondrial population with a full complement of nucleus- and mitochondrion-encoded gene products. Although mitochondrial fission inevitably generates organelles lacking nucleoids, fusion ensures that the mitochondrial genome and gene products are replenished before functionality is lost.

Cells defective in mitochondrial division contain highly interconnected net-like mitochondria that typically accumulate in restricted areas, leaving large parts of the cell devoid of mitochondria. Proper mitochondrial distribution depends on division to split the mitochondrial network into transportable units. Obviously, this is particularly important in large and extended cells, such as neurons. Accordingly, DRP1 and OPA1 are crucial to establish proper mitochondrial content and distribution in dendrites. This, in turn, is essential for the maintenance of dendritic spines and synapses, which are neuronal structures with a particularly high energy demand[26,25].

In other cell types, fused mitochondrial networks act as electrically united systems that transmit the membrane potential generated by the proton pumps of the respiratory chain[27]. This mechanism was proposed to play an important part in the dissipation of metabolic energy in muscle cells.

Hence, it seems that concerted activities of the mitochondrial fusion and fission machineries shape the mitochondrial compartment and adapt it to the specific requirements of the cells.

Furthermore research over the past decades leaves no doubt that mitochondria have a crucial role in ageing. The mitochondrial theory of ageing postulates that

the respiratory chain produces reactive oxygen species (ROS) as byproducts of oxidative phosphorylation. Because mitochondria are a major source for ROS, mtDNA is particularly vulnerable to ROS-induced mutations and lesions. As a result, gradual and progressive accumulation of mtDNA mutations leads to a loss of functional respiratory chain complexes, resulting in a decline of bioenergetic capacity and eventually age-associated pathologies and death[28]. Mitochondrial dynamics was proposed to counteract this detrimental process through two activities: rescue of non-functional organelles by fusion and elimination of damaged organelles after fission. Irrespective of the level of heteroplasmy, mitochondria showed a homogenous pattern of respiratory activity at the cellular level as a result of fusion and inter mixing of mitochondrial contents[29]. These suggests that fusion of mitochondria and complementation of mitochondrial gene products are a defence mechanism against cellular ageing.

Autophagy is a process of self-degradation of cellular components that are harmful or no longer required. damaged or surplus organelles or portions of cytosol are sequestered by double-membrane autophagosomes that fuse with lysosomes or vacuoles and are broken down by hydrolytic enzymes[30]. The autophagic breakdown of mitochondria is termed mitophagy. It is tempting to speculate that mitophagy constitutes a mechanism to remove dysfunctional mitochondria from the cell and thereby prevent proliferation of mutated mtDNA. Support for this hypothesis came recently from a seminal study that described the behaviour of fluorescently labelled mitochondria in cultured mammalian cells[31]. Mitochondrial division was found to frequently produce two uneven daughter organelles, one with high membrane potential and one with decreased membrane potential and reduced OPA1 levels. Intriguingly, mitochondria with decreased membrane potential and reduced OPA1 levels are less likely to be engaged in subsequent fusion events and, instead, are prone to removal by mitophagy. Remarkably, inhibition of fission decreases mitophagy and results in decline of respiratory capacity, whereas arrest of autophagy leads to the accumulation of mitochondria with low membrane potential and low OPA1. on the basis of these observations a hypothesis was proposed that integrates mitochondrial dynamics and turnover in the mitochondrial life cycle. Mitochondrial fission frequently generates solitary mitochondria that might either maintain an intact membrane potential and re-fuse with the mitochondrial

network, or might be depolarized and depleted of OPA1, thereby preventing further rounds of fusion. This enables subsequent elimination by mitophagy[31]. Therefore, mitochondrial division may contribute to a quality control mechanism that facilitates removal of damaged mitochondria from the cell.

At last mitochondrial fission is important for apoptosis. A key event in apoptosis is mitochondrial outer membrane permeabilization, which releases cytochrome-c and other pro-apoptotic factors from the intermembrane space into the cytosol to trigger downstream cell death pathways[32,33]. Regulation of apoptosis involves DRP1-dependent mitochondrial fragmentation in a wide range of organisms, including yeast[34], flies[35], worms[36] and mammals[37].

Although many issues remain controversial, it seems that mitochondrial fragmentation occurs early in the apoptotic pathway, just prior to or simultaneously with outer membrane permeabilization and before effector caspase activation. Further work is required to determine how the components of mitochondrial fission and fusion actively participate in programmed cell death.

1.2 Bioenergetics of mitochondria

The cellular energy currency, ATP, can be produced in 3 ways: (a) by anaerobic glycolysis (which takes place in the cytosol); when glucose is converted to pyruvate only a small fraction of total free energy potentially available for ATP synthesis is released with an overall net gain of 2 ATP molecules; (b) by tricarboxylic acid (TCA), also known as citric acid or Krebs cycle, which takes place in mitochondrial matrix and yields one ATP molecule percycle, (c) by oxidative phosphorylation (OXPHOS), which takes place in the IMM and allows~15 times more ATP to be made than that produced by glycolysis. This is because mitochondria house the major enzymatic systems used to complete the oxidation of sugars, fats and proteins that enter the Krebs cycle after being converted to acetyl-CoA. Pyruvate produced by glycolysis enters mitochondria, where pyruvate dehydrogenase catalyzes its conversion to acetyl-CoA, also reducing NAD+ to NADH; fatty acids are converted to acetyl-CoA by β oxidation; while various enzymes exist for the conversion of specific amino acids in to pyruvate, acetyl-CoA or directly into specific citric acid cycle intermediates. Once in the TCA cycle, CoA causes the acetyl moiety to react

with oxaloacetate to produce citrate. In a series of seven subsequent enzymatic steps, citrate is oxidized back to oxaloacetate while giving off two molecules of carbon in the form of CO2, three NADH and one of flavin adenine dinucleotide FADH2[38]. The latter two carry the free energy liberated from the Krebs cycle to the mitochondrial electron transport chain made up of OXPHOS complexes I to V (Figure 4).

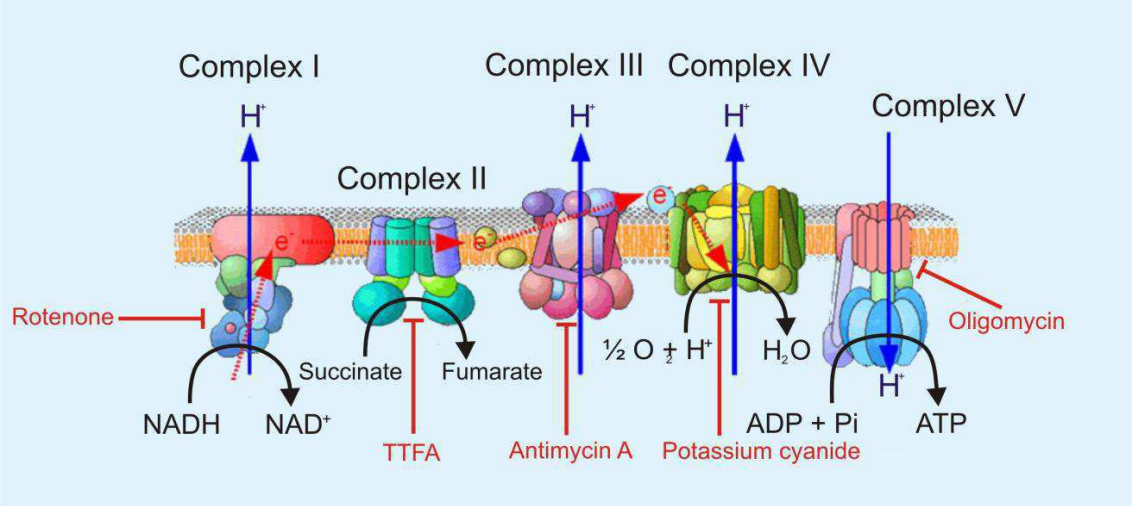

Figure 4. Cellular respiration: the electron transport chain and ATP synthase.
Complexes I-IV of electron transport chain (ETC) and the ATP synthase (Complex V) are embedded in the IMM. The ETC substrates coming from Krebs cycle feed the electrons to complexes I and II, electrons are then transferred along the chain due to the increasing redox potential of the OXPHOS enzymes. The flow of electrons is accompanied by proton pumping from the matrix to theintermembrane space creating the electrochemical proton gradient which then drives the synthesis of ATP. Complexes I to V can be inhibited by rotenone, thenoyltrifluoroacetone (TTFA), antimycin A, cyanide and oligomycin, respectively.

NADH donates electrons to respiratory complex I, also called NADH dehydrogenase, an L-shaped enzyme complex that contains a hydrophobic domain embedded in the IMM and a hydrophilic arm which protrudes into the mitochondrial matrix and contains the NADH binding site. The reduced cofactor donates two electrons to a flavin mononucleotide prosthetic group contained in the hydrophilic arm of complex I. These electrons are then passed down the arm via a series of iron–sulphur clusters to the lipid soluble redox carrier coenzyme Q (CoQ)[38]. The liberated energy is used to pump out four protons (H+) from the matrix to the IMS against their concentration gradient. The other cofactor formed in the citric acid cycle (FADH2) never leaves the complex, as the dehydrogenase itself is a part of the electron transport chain. The enzyme, also known as complex II, contains FAD as a prosthetic group alongside Fe–S

clusters to catalyze of electron transfer to ubiquinone (CoQ)[39]. In contrast to complex I, no protons are pumped by this complex as the liberated energy is insufficient. The electrons coming either from complex I or II reduce CoQ; the ubiquinone diffuses through the IMM to complex III, also called cytochrome c reductase. This enzyme oxidizes CoQ and passes the liberated electrons to two molecules of cyt c. In total four protons are translocated to intermembrane space – two coming from the oxidation of CoQ and two additional ones[40]. Finally electrons arrive to complex IV (cytochrome c oxidase) where they are passed to oxygen to form water. Again, alongside this reaction, four protons are pumped from the mitochondrial matrix into the intermembrane space[41].

Because the IMM is impermeable to H+ and charged species in general, the movement of protons across the inner mitochondrial membrane generates an electrochemical proton gradient or proton-motive force (ΔμH), which can be calculated with the Nernst equation:

$$\Delta\tilde{\mu}H = zF\Delta\Psi_m + RT\ln\frac{[H^+]_{in}}{[H^+]_{out}}$$

It can be appreciated that the ΔμH results from the sum of the pH difference and the membrane potential difference (ΔΨm), which is negative inside. ΔpH in mammalian cells is about 0.5-1 units, which corresponds to 30-60 mV; ΔΨm is in the order of 180-200 mV, which makes it the major component of the proton-motive force[42]. As suggested by Peter Mitchell in 1961[43], ΔμH is coupled to phosphorylation of ADP, which occurs at OXPHOS complex V, or ATP synthase. The enzyme consists of a membrane-spanning F_o domain, made of a variable number of c subunits organized in a ring-like structure. This proton-conducting ring allows proton influx back to the matrix, which results in F_o rotation. This is transmitted through a shaft to the F_1 portion, a matrix-exposed complex where conversion of ADP+Pi to ATP takes place. Of note, the ATP synthase can work in reverse, that is hydrolyze ATP and pump protons to intermembrane space when nΔμH is lower than the phosphorylation potential (ΔGp), where n is the H+/ATP stoichiometry[42].

Several studies showed that inhibition of respiratory chain complexes by drug treatment induces fragmentation of the mitochondrial network. This was

observed, for example, in HeLa cells[44, 45], CV1-4A cells[44, 46], mouse embryonic fibroblasts[46], human skin fibroblasts[47], cultured cortical neurons[47],MRC5 fibroblasts[48], and other cell types[49]. In contrast, some cell types retain filamentous mitochondria during respiratory chain inhibition, and the phenotypes of respiratory-deficient cells lacking an intact mitochondrial genome are ambiguous[49]. Mitochondria appear more elaborately interconnected and ramified in HeLa cells when mitochondrial respiration is induced by growth in galactose containing medium (in comparison to glucose medium)[50]. However, this effect was not observed in MRC5 fibroblasts[50]. In sum, the majority of the available data point to a functional link between changes of energy metabolism and adaptations of mitochondrial morphology in mammalian cells. It appears that interconnected mitochondrial networks are frequently present in metabolically and respiratory active cells, whereas small and fragmented mitochondria are more prevalent in quiescent and respiratory inactive cells[51].

Bioenergetic role of mitochondrial fusion

Mitochondrial fusion allows efficient mixing of mitochondrial content, and it generates extended mitochondrial networks. Both effects are advantageous under conditions of high energy demand, and disruption of mitochondrial fusion results in mitochondrial dysfunction and loss of respiratory capacity both in yeast and in mammalian cells[51-53].

Deletion of the FZO1 or MGM1 genes, encoding key components of the mitochondrial fusion machinery, leads to rapid loss of the mitochondrial genome in yeast[24]. As several respiratory chain subunits are encoded by the mitochondrial DNA (mtDNA), it is difficult to determine whether loss of fusion directly contributes to a decline of respiratory capacity, or whether respiratory defects infusion-deficient yeast mutants are an indirect consequence of a defect in mtDNA inheritance. Deletion of the DNM1 gene, encoding a key mediator of mitochondrial fission, extends life span in yeast[54]. It is not exactly known whether longevity is directly related to the highly fused, interconnected mitochondrial network characteristic for fission-defective yeast mutants, or whether it is linked to the inactivation of cell death pathways or other reasons. Furthermore, deletion of the MGM1 gene reduces life span in yeast[55], suggesting that mitochondrial fusion is beneficial for cell physiology. However, it remain sun known whether loss of mtDNA in *mgm1* mutants has an impact on

life span, and whether there is a direct link between mitochondrial fusion activity and respiratory capacity in yeast[51].

Content mixing and complementation of gene products in fused mitochondria were proposed to be crucial for maintenance of mitochondrial functions and counteract cellular aging. During the process of aging, different mutations accumulate in different mtDNA molecules. Thus, wild-type mtDNA coexists with different mutant alleles or deletions, a state termed heteroplasmy. When individual mitochondria have acquired mutations in different genes, each mitochondrion will be respiratory deficient. However, when these mitochondria fuse, each fusion partner contributes an intact allele, and complementation of gene products restores respiratory activity[56].

Several recent reports underscore the importance of mitochondrial fusion under conditions of high energy demand in mammals. It was shown that some cell stressors, including UV irradiation and several drugs that inhibit cytosolic protein synthesis, can trigger increased mitochondrial fusion in mouse embryonic fibroblasts, a process termed stress-induced mitochondrial hyperfusion. Mitochondria elongate and form a mesh of highly interconnected filaments in an Mfn1 and Opa1-dependent manner. Stress-induced mitochondrial hyperfusion is accompanied by increased mitochondrial ATP production. It is conceivable that fusion is necessary to optimize mitochondrial function in order to allow the cell to cope with increased energy demand during selective forms of stress[57].

Bioenergetic role of mitochondrial fission

Mitochondrial division serves a variety of different functions. These include partitioning and inheritance of the organelles during cell division, release of cytochrome c and other intermembrane space proteins during apoptosis, and generation of transportable mitochondrial units for movement along the cytoskeleton[1]. While these functions are not directly related to bioenergetics, it was proposed that mitochondrial fission also serves to eliminate damaged organelles from the mitochondrial network in order to allow their removal by autophagy. This activity supposedly constitutes an organellar quality control mechanism and contributes to maintenance of bioenergetic capacity[51, 5831, 51, 5831, 31, 51, 58].

The observation of fluorescently labelled mitochondria in cultured mammalian cells revealed that mitochondrial division frequently generates two uneven daughter organelles, one with high membrane potential and another one with decreased membrane potential. Strikingly, mitochondria with low membrane potential were found to have reduced levels of the inner membrane fusion factor Opa1, and thus are less likely to re-fuse with the mitochondrial network. Instead, these dysfunctional mitochondria are removed from the cell by autophagy[31]. Thus, mitochondrial fission followed by selective fusion provides a mechanism to segregate damaged and dysfunctional mitochondria and permit their degradation by autophagy. In the long term, this mechanism contributes to the maintenance of a healthy mitochondrial population and maintenance of bioenergetic capacity[31].

Adaptation of mitochondrial dynamics to bioenergetic conditions

What are the molecular processes that adapt the activities of the mitochondrial fusion and fission machineries to the bioenergetic state of the cell? At least three different, mutually non-exclusive mechanisms likely play important roles: first, the activity of the mitochondrial fusion machinery might directly respond to the bioenergetic state of mitochondria; second, several cellular signalling pathways modulate the activity of fusion and fission proteins; and third, the expression of key factors of mitochondrial dynamics is regulated at the transcriptional level[51].

Fusion and fission are antagonistic processes that predominate under different conditions to adapt mitochondrial morphology and dynamics to the bioenergetic requirements of the cell (Figure 5). Fused mitochondria are preferred when optimal mitochondrial function is needed. Thus, fused mitochondrial networks are frequently found in respiratory active cells. Apparently, mixing of the matrix and the inner membrane allows the constituents of the respiratory machinery to cooperate most efficiently. Furthermore, fusion engages the entire mitochondrial compartment in respiration to maximize ATP synthesis. It is conceivable that the sudden need for metabolic energy is the reason for the formation of hyperfused mitochondrial networks that are formed upon exposure of cells to stress, and that fusion optimizes mitochondrial function during starvation. While fusion in stress-exposed or starving cells constitutes a short-term adaptation to changing environmental conditions, it also plays a beneficial

role for maintenance of bioenergetic capacity in the long term. Upon aging, fusion allows complementation of gene products and thus compensates for the accumulation of mitochondrial mutations in heteroplasmic cells. Moreover, fused mitochondrial networks contribute to the dissipation of energy in large cells with a particularly high energy demand. In contrast, fragmented mitochondria are frequently found in resting cells and might represent a "default" morphological state when high respiratory activity is not required. The activity of the mitochondrial fission machinery contributes to maintenance of bioenergetic capacity as it allows the elimination of irreversibly damaged mitochondria by autophagy. The activity of the key proteins of mitochondrial dynamics is regulated at multiple levels, including transcription, post-translational modification, and direct response to the bioenergetic state of mitochondria[51].

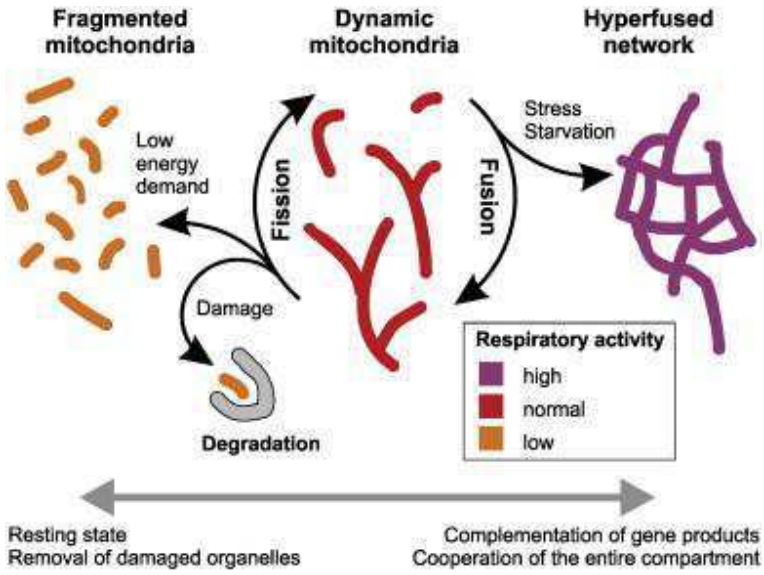

Figure 5. Model of adaptation of mitochondrial morphology to respiratory activity.
Fragmented mitochondria constitute the preferred morphological state when respiratory activity is low. Under respiratory conditions mitochondria undergo frequent cycles of fusion and fission to allow spreading of metabolites and macromolecules throughout the entire compartment. At the same time, mitochondrial fission is required for removal of damaged and inactive organelles by autophagy. When the bioenergetic state becomes critical, for example under nutrient deprivation or exposure to certain forms of stress, highly fused mitochondria are formed to optimize mitochondrial function[51].

1.2 Mitochondrial dynamics and disease

Defects in mitochondrial fusion and fission primarily affect neuronal functions, as nerve cells have a high energy demand and strictly depend on mitochondrial functions, and neurons are particularly sensitive to perturbations of mitochondrial distribution. Dysfunctions of mitochondrial dynamics are implicated in inherited and age-associated neurodegenerative diseases (table 1) [1].

Molecular defect	Disease	Neuronal defect
Mutations in *OPA1* that impede mitochondrial fusion	Autosomal dominant optic atrophy	Degeneration of retinal ganglion cells and optic nerve
Mutations in *MFN2* that impede mitochondrial fusion	Charcot–Marie–Tooth disease type 2a	Degeneration of long peripheral sensory and motor neurons
Mutations in *DRP1* that impede mitochondrial fission	Unnamed	Abnormal brain development, optic atrophy and neonatal lethality
Mutations in *PINK1* or *PARK2* that disturb mitochondrial dynamics	Hereditary early onset Parkinson's disease	Degeneration of dopaminergic neurons in the substantia nigra

DRP1, dynamin-related protein 1; *MFN2*, mitofusin 2; *OPA1*, optic atrophy protein 1; *PARK2*, Parkin.

Autosomal Dominant Optic Atrophy (DOA)

DOA is the most common inherited optic nerve disorder seen in clinical practice, the pathological hallmark of this disorder is preferential loss of the retinal ganglion cell (RGC) layer within the inner retina, which leads to optic nerve degeneration and subsequent visual failure[59]. DOA has an insidious onset, and it typically presents in early childhood with bilateral, symmetrical central visual loss and dyschromatopsia. Visual loss is invariably progressive, and almost all affected individuals will eventually fulfil the legal requirement for blind registration[60].

The majority (50–65%) of families with DOA harbour pathogenic mutations within the OPA1 gene, which consists of 30 coding exons spanning over 100 kb of genomic DNA[61]. OPA1 codes for a 960-amino-acid, dynamin-related GTPase that localizes to the inner mitochondrial membrane(Figure 6).

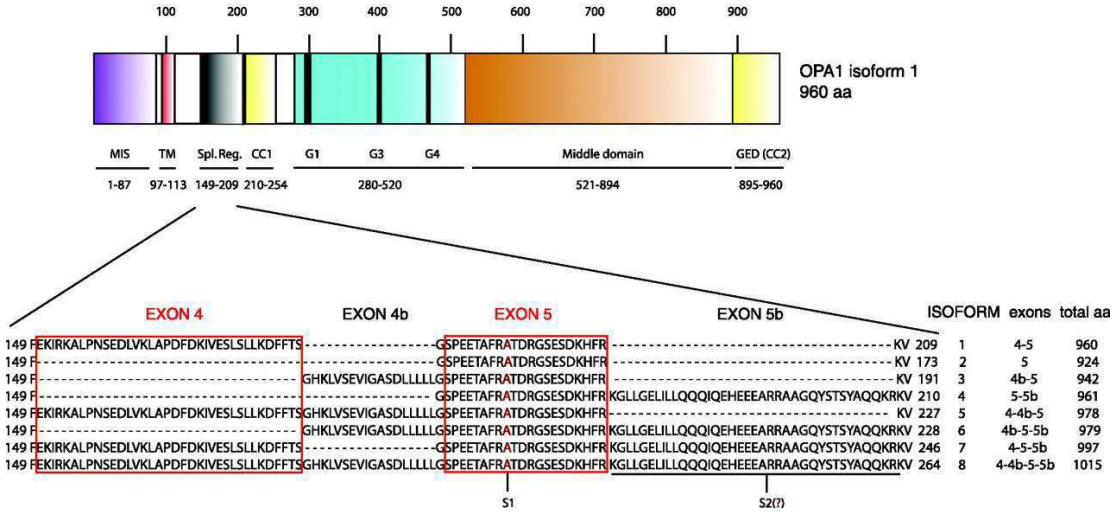

Figure 6: Domains and motifs identified in human OPA1. The GTPase domains are shown in blue with the distinct G motifs shown in black bars (from G1 to G4). Coiled-coil regions (CC) and/or GED (GTPase effector domain) are shown in yellow. The transmembrane domains (TM) are shown in red. The mitochondrial import sequence (MIS) is shown in purple, with the cleavage site of mitochondrial processing protease (MPP) in residue F88. The middle domain is colored in brown and the alternative spliced region (Spl. Reg.) in black. The length and topology in amino acids for each region and domain are shown. The primary sequence for each OPA1 splicing isoform is also depicted. The alternative splicing of exons 4, 4b, and 5b generates eight isoforms of OPA1 with distinct numbers of total amino acids. All OPA1 isoforms contain exon 5 with the S1 cleavage site (alanine). Exon 5b contains a second cleavage site S2, although the exact residue of this site has not been determined[62].

The gene is highly expressed within the RGC layer, although the protein is ubiquitous, and abundant levels have also been identified in photoreceptors and other non ocular tissues such as the inner ear and the brain[63]. Over 200 disease-causing variants have been reported so far in this highly polymorphic gene, with mutational hot spots in the catalytic GTPase domain (exons 8–15) and the dynamin central domain (exons 16–23)[64]. The majority of OPA1 mutations result in premature termination codons, and the resultant truncated mRNA species are highly unstable, being rapidly degraded by protective surveillance mechanisms operating via nonsense-mediated mRNA decay. Haploinsufficiency, therefore, is a major disease mechanism in DOA, and the pathological consequences of a dramatic reduction in OPA1 protein levels is

highlighted by those rare families who are heterozygous for microdeletions spanning the entire OPA1 coding region[65].

Progressive visual failure remains the defining feature of DOA but, with greater availability of genetic testing, a specific OPA1 mutation in exon 14 (c.1334G>A, p.Arg445His) has been found to have a particular predilection for causing sensorineural deafness[66,67]. The phenotypes associated with OPA1-linked disease have expanded even further to encompass a wide range of prominent neuromuscular features such as ataxia, myopathy, peripheral neuropathy, and classical chronic progressive external ophthalmoplegia (CPEO)[68]. These so-called DOA+ variants are mechanistically relevant, as they highlight the deleterious consequences of OPA1 mutations not only for RGCs, but also for other CNS populations, peripheral nerves, and skeletal muscle.

Although DOA+ was only recently recognized as a distinct clinical entity, up to 20% of OPA1 mutation carriers are now thought to be at risk of developing DOA+ features, which has major implications for patient counselling[69]. Furthermore, OPA1 screening is increasingly performed as part of diagnostic panels for patients with unexplained neurodegenerative disorders, and other hitherto unreported pathological manifestations are bound to emerge[70].

It remains unclear why Opa1-DOA manifests with an apparently restricted clinical ocular phenotype, comprising retinal ganglion cells (RGC) loss. OPA1 is ubiquitously expressed throughout the body: in the heart, skeletal muscle, liver, testis, and most abundantly in the brain and retina. In the human retina, OPA1 is present in the cells of the RGC layer, nerve fibre layer, the photoreceptor layer, and the inner and outer plexiform layers (IPL & OPL). A plausible hypothesis as to why RGC neurons may be more vulnerable to OPA1 inactivation could be a particular susceptibility to mitochondrial membrane disorders inducing mitochondrial dysfunction or mislocalization. Indeed, reports describe altered mitochondrial ATP synthesis and respiration in OPA1-inactivated cells[66]. Moreover, recent studies show the effect of mitochondrial morphology regulation on mitochondrial distribution in neurons and their contribution to dendrite formation and synaptic plasticity[21]. This could be of particular importance in RGC neurons that display a specific distribution of mitochondria in the cell body, myelinated and unmyelinated axons. Additionally,

the defects in DOA can be ascribed to the loss of the crucial control exerted by OPA1 on the structural organization of the cristae and apoptosis[71,21].

1.3 *Drosophila* as a model organism

Ever since Morgan isolated the white mutation in *Drosophila melanogaster* in 1910, the tiny fruit fly has made large contributions to the understanding of the genetic and molecular mechanisms of heredity and development. More recently, the remarkable power of fruit fly genetics has been applied to study the basic mechanisms of human diseases, including those debilitating pathologies that affect the human brain.

There are several reasons why *Drosophila m.* is widely used as models of human diseases. The first and foremost reason is based on the presumption that fundamental aspects of cell biology in flies have been conserved throughout evolution in higherorder organisms such as humans[72]. A report demonstrating that approximately 75% of the disease-related loci in humans have at least one Drosophila homologue confirms the high degree of conservation present in flies. Furthermore, studies of developmental events in the fly and subsequent similar studies in higher animals have revealed a stunning degree of functional conservation of genes. These studies indicate that not only basic cell biology but also higher-order events such as organ “construction” and function are conserved.

Drosophila has an unrivalled battery of genetic tools including a rapidly expanding collection of mutants, transposon-based methods for gene manipulation and systems that allow controlled ectopic gene expression and balancer chromosomes[73]. It should be possible to target endogenous wild-type copies of "disease gene" in the fly genome for inactivation (knock-out); defined mutations can also be "engineered" (knock-in) into respective endogenous genes, to create gain-offunction models[74].

The above characteristics of such a minuscule system model, combined with the rapid generation time, inexpensive culture requirements, large progeny numbers produced in a single cross and a small highly annotated genome devoid of genetic redundancy, are poised to yield seminal insights into human disease[73].

For almost a century, fruit flies have been providing a useful tool to study various different subjects: form the chemical basis of mutagenesis, to the definition of genes, from developmental biology, to animal behaviour. The ability to use Drosophila as a powerful tool to approach pathogenetic disease mechanisms for human diseases speaks to a tremendous application in biomedical research[74].

Mitochondrial dynamics in *Drosophila*

Thanks to the use of animal models, we are starting to understand how this leads to neuronal dysfunction and loss, the interplay between mitochondrial shape and function is extremely complex and the current discovery rate is slowed down by the complexity of murine models. A valid alternative is represented by *Drosophila melanogaster* that has been successfully employed to lay the basis for several key findings in the field of neurodegeneration.

Mitochondrial shape in living cells is very heterogeneous and can range from small spheres to interconnected tubules. The morphological plasticity of mitochondria results from the ability of this organelle to undergo fusion and fission, which are regulated by a family of mitochondrial shaping proteins.

As described above, mitochondrial fusion is promoted by large trans-membrane dynamin-related proteins. OPA1 resides in the inner mitochondrial membrane and is involved in mitochondrial fusion, as well as in the regulation of cristae biogenesis and remodeling. In *H. sapiens*, 8 different OPA1 isoforms are retrieved, which are differentially post-translationally processed in at least five different protein forms by a complicated and yet not completely understood network of proteases that include iAAA, mAAA, paraplegin, Oma1,and Parl; the concerted action of these proteases results in the production of long and short forms of the protein that are both required for correct function of the protein and therefore for mitochondrial fusion, as well as of a soluble form that albeit quantitatively scarce, participates in the formation of the OPA1-containing oligomers that stabilizes the cristae during apoptosis[75].

Drosophila OPA1 homologue (*dOPA1*) shares 51.2% similarity with the human orthologue. In fruitflies, Opa1 gene is transcribed into 2 isoforms, that are processed into a short form by *Drosophila* presenilin-associated rhomboid-like (PARL) homologue rho-7, a protease that is conserved during evolution from yeast to mammals. Most studies on *dOPA1* analyzed mutant flies where the

function of the protein had been ablated by a genomic P-element/transposon insertion[75] and recently it was also reported that downregulation of *dOPA1* in the heart results in dilated cardiomyopathy, with severe alteration of contractility[76].

In addition to OPA1, all the main mammalian mitochondria-shaping proteins are highly conserved between *Drosophila* and *Humans* (Table 2), supporting the potential role of flies as a model of primary defects of mitochondria dynamics.

Protein	Domains	*Drosophila* homologue	Expression data in post-embryonic organs or tissues	Phenotypes	Disease
OPA1	GTPase, GTPase effector (GED)	Opa1-like, CG8479	adult eye, adult central nervous system, larval/adult hindgut, larval/adult fat body, adult spermathecae	Lethality, cardiomyopathy, Rough and glossy eye	Autosomal Dominant Optic Atrophy (ADOA)
MFN2, MFN1	GTPase, Heptad repeats (HR)	Marf, Mitochondrial assembly regulatory factor, CG3869	adult head, adult eye, adult central nervous system, adult crop, larval/adult midgut, larval/adult hindgut, larval/adult Malpighian tubules, adult heart, adult fat body, adult salivary gland, larval trachea, adult spermathecae, adult male accessory gland, larval/adult carcass	Lethality, cardiomyopathy	Charcot–Marie–Tooth type IIa (CMT2A)
DRP1	GTPase, GED	Drp1, CG3210	larval/adult central nervous system, larval Malpighian tubules, larval salivary gland, adult testis	Lethality, Defective Nebenkern, Mitochondrial distribution, Impaired neurotransmission	Alzeheimer's, Huntington's, ADOA, CMT2A
FIS1	tetratricopeptide repeat(TPR)-like motifs	Fis1, CG17510	adult head, adult eye, larval/adult central nervous system, adult crop, larval/adult midgut, larval/adult hindgut, larval/adult Malpighian tubules, adult heart, larval/adult fat body, larval/adult salivary gland, larval trachea, adult female reproductive system, adult male reproductive system, larval/adult carcass	Mitochondrial dynamics	
MFF	DUF800	Tango11, CG30404	larval/adult central nervous system, larval Malpighian tubules, larval fat body, larval salivary gland, adult ovary	Mitochondrial and peroxisomes fission	

Table 2: Mitochondria-shaping proteins in D.melanogaster. Mammalian mitochondria-shaping proteins and their respective Drosophila homologues are listed. The main functional domains, expression in different fruitfly's organs and tissues, observed phenotypes and disease to which proteins are related are described.

Drosophila as a model of primary defects of mitochondrial dynamincs: DOA and OPA1

The main proof of the pivotal role of mitochondria dynamics in neurodegeneration comes from the linkage between mutations in genes codifying mitochondrial shaping proteins and neurological disorders.

The analysis of the genetic mechanisms causing neurodegenerative disorders requires the use of a model organism where symptoms and signs can emerge, where many individuals can be analyzed to generate statistically significant categories of phenotypes, where the aging associated progressive degeneration can be followed and molecularly investigated.

The most common cause of DOA are mutations in OPA1. More than 100 different mutations spread throughout the OPA1-coding sequence are described so far, and most of them are localized in GTPase domain and in the 3′ end of the coding region and cause premature truncation of the protein. Alignment of protein sequence of human OPA1 with the Drosophila homologue

shows that the domains most subjected to pathogenic mutations are well conserved (Figure 7)[75].

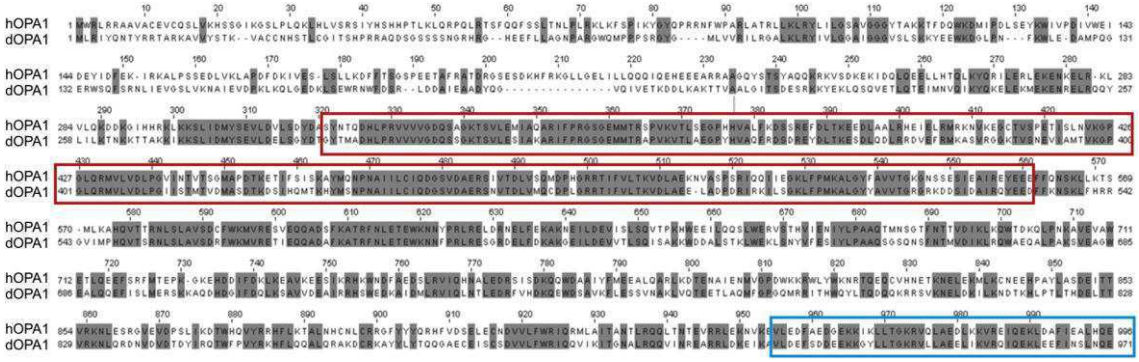

Figure 7: Protein sequence alignment between human OPA1 (hOPA1) and Drosophila OPA1 (dOPA1). Identity is highlighted in gray, GTPase domain in red and amino acids codified by exons 27 and 28 in blue.

Although apparently different, humans and flies are very similar in crucial aspects. Key molecular pathways required for the development of a complex animal, such as patterning of the primary body axes, organogenesis, wiring of a complex nervous system and control of cell proliferation are highly conserved between flies and vertebrates, then *Drosophila melanogaster* represents a powerful and useful model to study DOA. Recent studies highlighted that heterozygous mutations of OPA1 in *Drosophila* do not show defective eye formation, but results in reduction of life span, abnormal mitochondria morphology and increase ROS production in whole body[77]. Even if eyes have no gross phenotype, mutated *opa1* flies show visual alterations in phototaxis with age-dependent progressive reduction of on/off transients in electroretinograms (ERG)[78]. Given lethal phenotype of homozygous mutations of Opa1 in the fruitfly, Drosophila were generated carrying homozygous mutant somatic clones in the eye[10]. Mosaic–eyes were rough and glossy indicating dysregulation of apoptosis and defective deposition of lens and pigments. In both whole body mutant and mosaic mutant-eyes flies, antioxidants were used to rescue phenotype. The use of Drosophila allowed to identify an important role for ROS in the dysregulation of eye and whole body functions and possibly in the pathogenesis of DOA, but many aspects still remain obscure, claiming for further investigation.

Two main approaches can be used in *D. melanogaster* to create a model for human disease. First, 'forward-genetic' approaches can be applied. Usually, mutagenizing agents or transposable elements are used to generate a large-

scale number of mutant flies. Screenings for the desired disease phenotype (for example, brain degeneration) are set up. Once the desired mutant flies have been selected, one can proceed to the identification of mutant genes, presumably involved in the generation of the phenotype of interest. Human homologues of the identified Drosophila gene products are plausible candidates for involvement in the disease that is being investigated. Many disease models were developed through this approach[79].

Alternately, when the disease genetic agent is known, 'reverse genetics' can be applied. Overexpression of dominant negative mutation or downregulation of a gene product may be used to screen for genetic interactors, after identification of a "scorable" phenotype (such as alteration of organization of cells in the eye). This approach is accomplished thanks to The Vienna Drosophila RNAi Center (VDRC), a joint initiative of the Institute of Molecular Biotechnology (IMBA) and the Research Institute of Molecular Pathology (IMP), which developed a *Drosophila* transgenic RNAi library. Moreover, the use of the binary system GAL4/UAS is a major tool in reverse genetics, because it allows the ectopic expression of a transgene in a specific tissue or cell type. Geneticists created genetic varieties of fruit flies, called GAL4 lines, each of which expresses the yeast transcriptional activator GAL4 in some subset of the fly's tissues.

In this work I generated a new *opa1* mutant in *Drosophila* using the new genome editing system CRISPR/Cas9.

1.4 Genome Editing in *Drosophila*

The advent of genome sequencing and genome-wide technologies for study of gene expression, polymorphism and regulation has revolutionalised our ability to associate genes with particular cellular functions or disease states. They have also allowed us to make predictions about the function of a large proportion of both coding and non-coding sequences. Although various techniques such as homologous gene targeting have allowed us to selectively mutagenise or alter gene function in a desired manner, the difficulty of applying these techniques on a large scale has restricted our ability to test hypotheses generated from such genome-wide analyses[80].

Genome editing technologies have been developed over the past decade that allow us to selectively mutagenise specific regions of the genome, and allow sophisticated and detailed mechanistic studies to be performed in a variety of organisms including *Drosophila*[81]. These technologies rely on specific DNA binding factors that can be used to target various functional domains to defined regions of the genome. Most experiments have used these reagents to generate a double strand break (DSB) in the DNA at the target site, that can then be repaired by nonhomologous end joining (NHEJ) or homologous recombination (HR)[82]. NHEJ is somewhat errorprone, and can result in the deletion or insertion of a few bases at the cut site, resulting in mutation of the DNA[82]. HR normally results in precise repair from the sister chromatid, but if an excess of a desired homologous template is supplied, this may be used to introduce defined changes in the underlying DNA[62,83].

CRISPR/Cas9 system

The clustered regularly interspaced short palindromic repeat (CRISPR/Cas9) system acts as a bacterial defense system against invading viruses and plasmids in many different bacterial species[84-87]. The best studied system is that from Streptococcus pyogenes. Here, the Cas9 endonuclease is targeted to sequences from the invading pathogen by a crRNA (CRISPR RNA), that provides specificity to the endonuclease by base pairing with a 20 nt complimentary sequence within the DNA[88, 89].

Endogenously, a further component, known as the tracrRNA (trans-acting crRNA) forms a complex with the crRNA and targets its incorporation into the

Cas9 complex. Recently, this system has been shown to work in many other organisms, including mammalian[90, 91], insect[92,93], plant[94] and fungal[95] cells. Fusion of the crRNA and tracrRNA into a ~100 nt synthetic single guide or chimeric RNA (sgRNA or chiRNA) has further simplified this system, which then only requires two components to be expressed[89, 90]. The specificity is determined by a 20 nt sequence at the 50 end of the sgRNA, which can be altered to match any desired sequence in the DNA. The only limitation upon this targeting is that the 20 nt guide sequence has to be followed by a protospacer adjacent motif (PAM) of NGG in the DNA in order for efficient cleavage to occur (Figure 8)[96]. This sequence should occur on average every 8 bases in the DNA, but recent reports have suggested that this requirement may be relaxed to include NAG sequences[97], increasing the number of potential target sites still further. CRISPR systems from other bacterial species have different PAM requirements[98, 99] and this suggests that it will be possible to engineer Cas proteins to bind to essentially any sequence in the future.

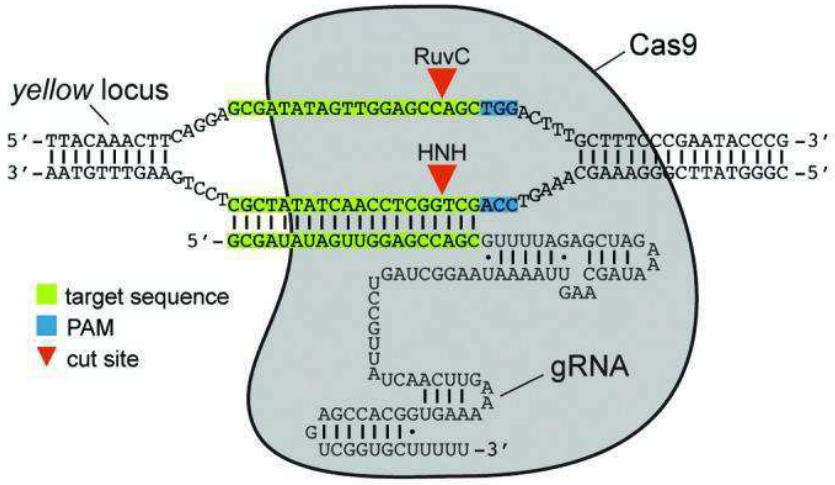

Figure 8: Schematic of the 2-component CRIRISPR/Cas9 system. A target site in the yellow locus is shown as an example. Cas9 is guided to a cleavage site by a chimeric RNA containing critical crRNA and tracrRNA sequences, including 20-nt of homology to a target site. This RNA has alternately been referred to as a guide RNA (gRNA), a single-guide RNA (sgRNA) or a chimeric RNA (chiRNA). Cas9 (gray) contains 2 distinct endonuclease domains, a HNH domain and a RuvC-like domain, that independently cleave both stands at the target site to generate a DSB (red arrowheads). Cleavage of target sites requires a high degree of homology to the gRNA and a 3-bp PAM (NGG) immediately 3′ of the target sequence.

Drosophila CRISPR system

Several groups have used the CRISPR/Cas9 system to induce targeted mutations in *Drosophila*[93, 96, 100-102], but differ in their approach to supplying the Cas9 protein and sgRNA components of the system. The first description of mutagenesis with CRISPR/Cas9 involved coinjection of two plasmids into syncytial blastoderm stage *Drosophila* embryos[96]. One plasmid expresses the Cas9 gene under the *Hsp70* promoter, and the second produces the sgRNA, driven by a *pol III* promoter from the *U6* gene. This was tested at the *yellow* gene, and resulted in mutagenesis of the gene that was capable of being transmitted to subsequent generations. The efficiency of mutagenesis due to inefficient NHEJ was fairly low, with 5.9% of the injected flies giving rise to at least one mutant offspring[96]. However, the authors further demonstrated that if two sgRNAs are supplied, targeting either end of the *yellow* gene, this can result in deletion of the intervening sequence, and that integration of short sequences at the cleavage site is possible by coinjection with a short single stranded oligonucleotide donor sequence[96].

A second technique that has been applied by two groups independently involves coinjection of *in vitro* transcribed Cas9 mRNA and sgRNA into early stage embryos, and achieves much higher mutagenesis rates due to inefficient NHEJ[93, 100]. Bassett et al. showed that up to 88% of injected flies gave rise to mosaic expression of the yellow gene implying that this technique is highly efficient. A second study by Yu et al. showed a similar efficiency (80%) at the *yellow* gene, but also showed successful mutagenesis at six other target loci spread throughout the genome, demonstrating the general applicability of this approach. The difference in efficiency between plasmid and mRNA injection techniques may be explained by the expression levels of the Cas9 protein and sgRNA, or by the timing of expression relative to the specification of germ cells in the embryo.

A third system has also been developed whereby two transgenic flies are produced, one expressing Cas9 in the germline under the *nanos* promoter, and a second with ubiquitous expression of the sgRNA again driven by the U6 promoter[103]. When these two flies are crossed together, highly efficient mutagenesis can be achieved, giving rise to up to more than 90% of flies with at least one mutant offspring, and allowing longer deletions of up to 1.6 kb to be

made efficiently by coexpression of two sgRNAs. Although efficient, this requires the time consuming step of producing a new transgenic fly for each sgRNA required, and removal of the Cas9 and sgRNA transgenes after mutant generation. However, this technique will have advantages in certain applications, since it is more reproducible than the techniques involving embryo injection.

The final technique uses injection of plasmids encoding the sgRNA into transgenic lines in which Cas9 is expressed specifically in the germline under the *vasa*[102] or *nanos*[104] promoters. These techniques avoid potentially problematic somatic mutagenesis by limiting Cas9 expression to the germline cells. Sebo et al. demonstrated high rates of mutagenesis in the G1 offspring derived from flies injected with plasmids encoding sgRNAs, but a significant proportion of the injected flies were infertile. By using the *nanos* promoter to drive Cas9 expression, Ren et al. achieved higher rates of fertility, and generated high rates of mutagenesis in G1 offspring.

In addition to the injection of vectors expressing guide RNAs (gRNAs), the production of fly lines that express Cas9 either ubiquitously or in the germline will also allow direct injection of *in vitro* transcribed sgRNA into these embryos. However, the relative efficiency of this technique has not been established.

Recently, expression vectors for Cas9 expression in *Drosophila* cell lines have also been described. The *Actin5c* and U6 promoters were use to drive expression of the Cas9 and sgRNA components, respectively. This results in highly efficient mutagenesis inmore than 80%cells due to the indels generated by inefficient NHEJ. The authors also demonstrated that homologous integration is possible using short oligonucleotide donors to insertsmall sequences, or longer homology arms to insert a 1.8 kb cassette at up to 4% efficiency[92].

Application of CRISPR/Cas9 system

The majority of applications of CRISPR/Cas9 in genome engineering use its ability to introduce DSBs at specific sites within the genome. The DSBs can be repaired by either NHEJ or HR, and both repair mechanisms can be used to generate mutations and manipulate the genome in a defined manner (Figures 9 and 10).

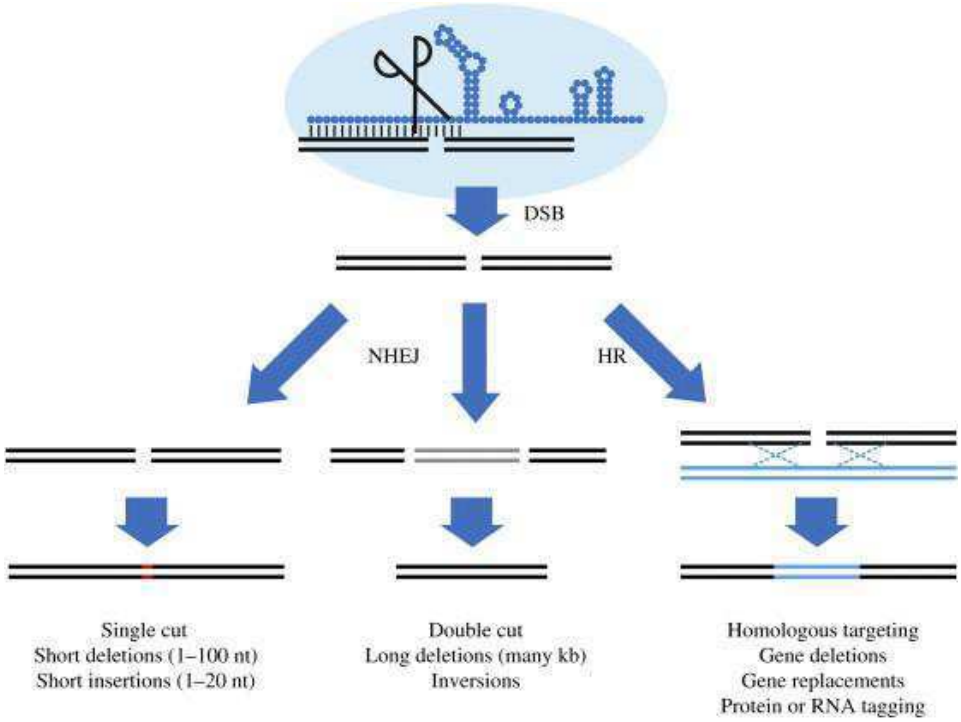

Figure 9 Double strand break repair can be used to target defined genomic changes. The double strand break (DSB) induced by the Cas9/sgRNA complex can be repaired by non-homologous end joining (NHEJ) or homologous recombination (HR). This can result in small insertions or deletions at the target site (left), deletions of larger genomic regions when two cuts are made (middle) or homologous repair with a desired template (right). This can be used to alter the genome in a variety of different ways (bottom).

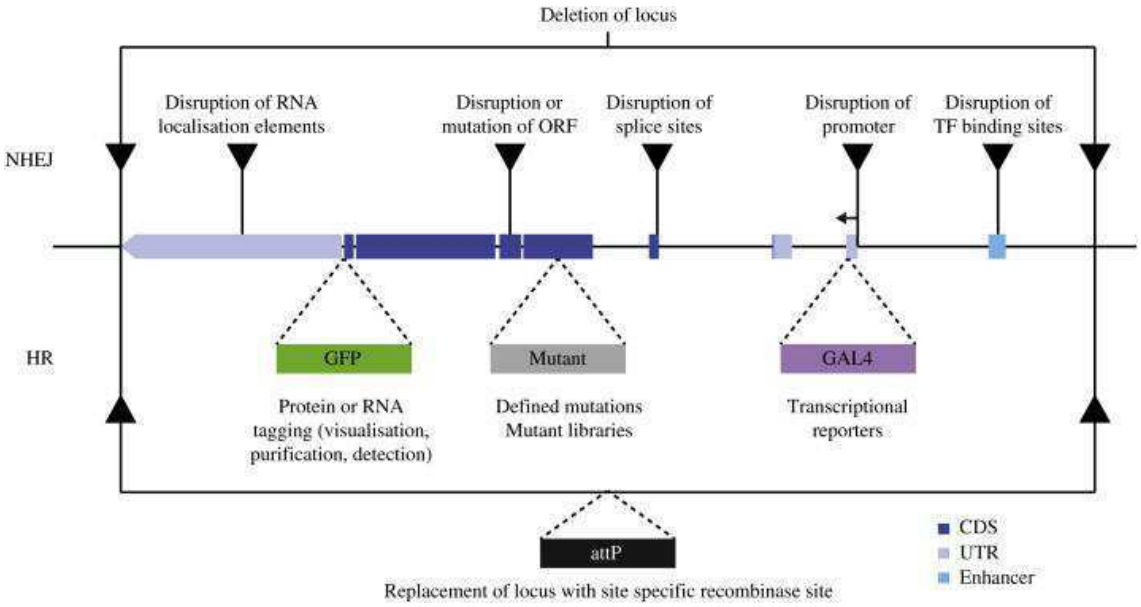

Figure 10 Uses of genome editing within protein coding genes. NHEJ repair (top) of Cas9-induced DSBs can be used to remove functional elements or disrupt genes in a variety of different ways. HR repair (bottom) can be used to insert or replace sequences present within the gene for a variety of different uses. Exons are indicated as boxes, with coding sequence (CDS) in dark blue and untranslated region (UTR) in grey. Enhancers are also indicated in light blue.

Creation of a DSB increases the rate of homologous repair at that site by several orders of magnitude[105], and this enables gene targeting to produce defined genetic changes much more rapidly and quickly than with classical techniques[106] (Figure 9). This relies on supplying a large excess of a homologous repair template with the desired changes[107]. The donor DNA can take two forms: single stranded DNA (ssDNA) oligonucleotides synthesised up to 200 nt in length and used to integrate short sequences, or longer double stranded DNA (dsDNA) constructs containing hundreds to thousands of nucleotides of homologous sequence on either side of the DSB site[107]. The latter are capable of integrating longer sequences at higher efficiency (Figure 10-11)[80, 108].

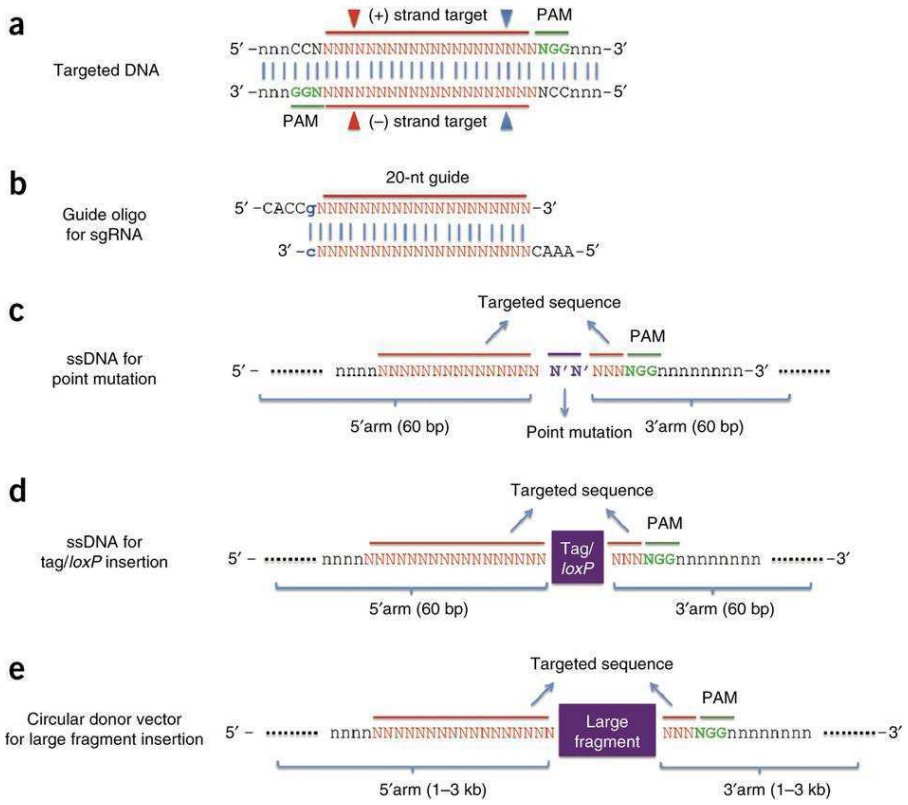

Figure 11: (a) Targeted DNA sequence consists of the DNA target (red bar) directly upstream of a requisite 5′-NGG adjacent motif (PAM; green). Cas9 mediates a DSB ~3 bp upstream of the PAM for (+) strand (blue triangle) or (−) strand (red triangle). **(b)** The guide oligos contain overhangs for ligation into the BbsI sites in px330, a G-C base pair (blue) added at the 5′ end of the guide sequence for T7 transcription and the 20-bp sequence preceding 5′-NGG in genomic DNA. **(c)** ssDNA for point mutation consists of a point-mutation site (purple), flanked by 60 base sequences on each side adjoining the DSBs. **(d)** ssDNA for tag/loxP insertion consists of tag/loxP site (purple), flanked by 60-bp sequences on each side adjoining the DSBs. **(e)** A circular donor vector for large fragment insertion consists of a large fragment, flanked by homology arm sequences on each side adjoining the DSBs.

2.AIM OF WORK

For a century, *Drosophila* has been a favored organism for genetic research. However, the array of materials and methods available to the *Drosophila*, worker has expanded dramatically in the last decade. Genetic engineering techniques have been optimized for studying several disease including defects of mitochondrial dynamics and thus also Dominant Optic Atrophy.

In this work I used the CRISPR/Cas9 system to generate the only mutant of DOA which can be helpful to understand the pathogenesis of this disease.

As describe above we generated two different *dOPA1* mutants: OPA1 *R417H*, a mutant that carries in endogenous dOPA1 gene the mutation corresponding to R445H in humans; and OPA1^{null} carrying a microdeletion leading to production of a inactive truncated protein of 482 amino acids.

We described the phenotypic effects observed in these mutants to determined if they have pathological features. We also analyzed the mitochondrial morphology in the nervous and muscular systems using confocal microscopy and the mitochondria functions through biochemical assays.

3.METHODS

3.1 Molecular Biology

Production of the chiRNAs

We chose the target PAM site NGG using the online tool http://tools.flycripr.molbio.wisc.edu/targetFinder/. The sequence adjacent to the PAM sites was used to cloned into pU6-BbsI-chiRNA.

We have done synthesize the oligos with BbsI site by Bio-Fab Research:

- *5'gRNA*: Sense oligo CTTCGGAGTTCCGAATGAAGGCGT
  Antisense oligo AAACACGCCTTCATTCGGAACTCC
- *3'gRNA*: Sense oligo CTTCGTCATCCT TTCGTCCACGAC
  Antisense oligo AAACGTCGTGGACGAAAGGATGAC

For annealing the oligos were diluted in TE or 1X ligation buffer, then the following program was run in a thermocycler 95°C for 5 min, than ramp to 25°C at a rate of -5°C/min.

The pU6-BbsI-chiRNA plasmid was cut with BbsI and de-phosphorylated finally the annealed oligos were ligated into the cut pU6-BbsI-chiRNA and the ligation transformed in E.Coli.

Production of the donor plasmids

The two dsDNAs were synthesize by Eurofins Genomics, these fragments have the following sequence:

dsDNA OPA1_R417H

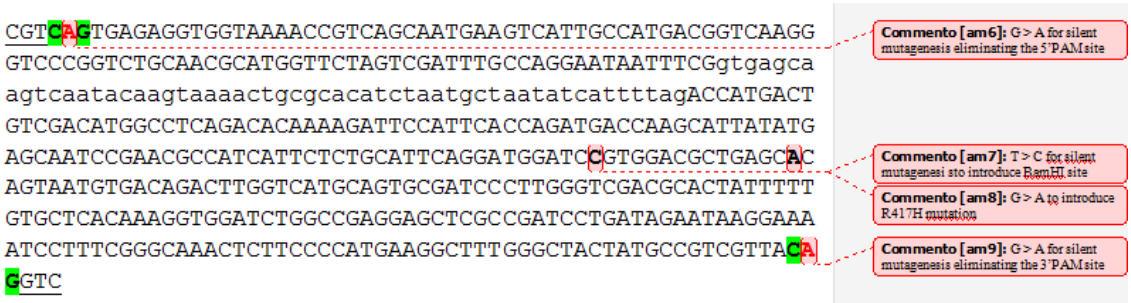

dsDNA OPA1^{null}

The synthesized dsDNA fragments and the 5' and 3' homology arms (1500bp) necessary for efficient homologous integration were assembled into pBluescript II SK+ using *Gibson Assembly® Cloning Kit* (NEB#E5510S). The homology arms were produced by PCR on *Drosophila* genomic DNA.

We used the web tool, *NEBuilder®* available at *www.NEBGibson.com*, to design the following PCR primers with overlapping sequences between the adjacent DNA fragments and for their assembly into cloning vector.

	Overlaps	Oligo (Uppercase = gene-specific primer)	Anneals	F/R	3' Tm	3' Ta *
Frag. 1	BSSK	acggtatcgataagcttgatACCGGTGAGAGACCACGC	5'_homology	Fwd	66.6°C	62.1°C
	OPA1	ctcactgacgCCTTCATTCGGAACTCCAC	5'_homology	Rev	62.1°C	62.1°C
Frag. 2	5'_homology	cgaatgaaggCGTCAGTGAGAGGTGGTAAAAC	OPA1	Fwd	62.4°C	62.1°C
	3'_HOMOLOGY	tttcgtccacGACCTGTAACGACGGCATAG	OPA1	Rev	62.1°C	62.1°C
Frag. 3	OPA1	gttacaggtcGTGGACGAAAGGATGACAG	3'_HOMOLOGY	Fwd	60.7°C	60.7°C
	BSSK	ccgggctgcaggaattcgatGTCGTGCACGAACCGATC	3'_HOMOLOGY	Rev	65.6°C	60.7°C

* 3' Ta (recommended annealing temperature) is calculated for the gene-specific portion of the primer for use with the selected PCR polymerase.

Screening of adults for mutation

Each genomic DNA extracted was used as template in a PCR reaction performed with primers designed to amplify a fragment of dOPA1 carrying the mutation.

Primers for screening: Forward GGGACCATTTAAAGTGAGAGAT

Reverse GTCGTGCACGAACCGATCCT

Components of single PCR screening reaction	*Volume reaction 50µl*
• *Phusion® High-Fidelity DNA Polymerase (2U/µl)*	0.5µl
• *5X Phusion HF Buffer*	10µl
• Genomic DNA template	2µl
• Forward Primer, 10µM	1µl
• Reverse Primer, 10µM	1µl
• 10mM dNTPs	1µl
• DMSO	1µl
• 50mM $MgCl_2$	0.5µl
• H_2O	to 50µl

PCR cicle

Cicle steps	*Temperature*	*Time*	
Initial denaturation	98°C	30''	
Denaturation	98°C	10''	30 cycles
Annealing	60°C	20''	
Extension	72°C	1'21''	
Final Extension	72°C	10'	

The fragment produced by PCR was digested with BamHI restriction enzyme in the following reaction:

Components	*Volume reaction 50µl*
Fragment of PCR (50ng/µl)	10µl
FastDigest BamHI enzyme (10U/µl)	1µl
10X FastDigest Buffer	5µl
H_2O	to 50µl

Mixed products were incubated at 37°C for 20 minutes and separated by electrophoresis through a 1% agarose gel. If a BamHI is present, two fragments at 955bp and 1764bp are visible instead of a single 2719bp fragment. After identification by restriction digest, mutants were confirmed by direct DNA sequencing.

Transformation of chemiocompetent cells

We transformed competent cells NEB 5-alpha Competent E. coli (High Efficiency, NEB #C2987) following the protocol:

- Thaw chemically competent cells on ice.
- Add 2 µl of the chilled assembly product to the competent cells. Mix gently by pipetting up and down or by flicking the tube 4–5 times. Do not vortex.
- Place the mixture on ice for 30 minutes. Do not mix.
- Heat shock at 42°C for 30 seconds. Do not mix.
- Transfer tubes to ice for 2 minutes.
- Add 950 µl of room-temperature SOC media to the tube.
- Incubate the tube at 37°C for 60 minutes. Shake vigorously (250 rpm) or rotate.
- Warm selection plates to 37°C.
- Spread 100 µl of the cells onto the selection plates. Use Amp plates for positive control sample.
- Incubate overnight at 37°C.

***Drosophila* genomic DNA extraction protocol**

- Obtain 1-5 flies per tube and keep on ice
- Add 100µl of Buffer A and grind with tissue grinder ~5 min
- Incubate at 65°C for 30 min
- Add 200µl of Buffer B
- Incubate on ice for 1 hour
- Centrifuge at 12000 rpm for 15 min
- Transfer supernatant to a new eppendorf tube
- Add 150µl of Isopropanol
- Centrifuge at 12000 rpm for 15 min
- Remove supernatant
- Wash with 200µl of cold Ethanol 70%
- Centrifuge at 12000 rpm for 15 min
- Remove supernatant
- Dry the pellet and resuspend in 30µl of H_2O
- Add 1µl of RNase

3.2 *Drosophila* genetics

Embryo injection

The plasmids were sent to BestGene Inc. for *Drosophila* embryo injection. The line *vas-Cas9-III* (BDSC#51324) was chosen for microinjection.

Generation of stable stocks

Individuals of the F2 carrying the *dOPA1* mutation and the SM6a balancer chromosome, were crossed to generate the stable mutant lines OPA1_R417H/SM6a and $OPA1^{null}$/SM6a. the stable mutant lines were crossed to generate other two lines OPA1 R417H/CyoGFP and $OPA1^{null}$/CyoGFP.

***Drosophila* strains used**

- elav-Gal4
- D42-Gal4
- UAS-mito-GFP (Bloomington Drosophila stock center)
- Control genotypes was W^{1118}

3.3 Microscopy

Immunohistochemistry

Immunostaining was performed on wandering third instar larvae raised at 25°C. After harvesting larvae, they were dissected dorsally in standard saline and fixed in 4% paraformaldehyde for 10 min and then washed in PBS containing 0.3% Triton-X and incubated overnight at 4°C with Goat Anti-Horseradish Peroxidase HRP antibody conjugate with Cyanine Cy™3 red (dilution 1:500, product by Jackson ImmunoResearch, Amax: 550nm, Emax: 570nm). Preparations were then washed 3 time in PBS. Coverslips were mounted with a drop of Mowiol mounting medium (Sigma).

Live imaging of mitochondrial network on muscles of *Drosophila* larvae

Experimental larvae were dissected dorsally in HL3 solution containing 7µM Glutamate, in order to reduce muscle contractions. After the larvae were incubated 30min at RT with MitoTracker® Orange CMTMRos 0.5µM in HL3 (Mitochondrion-Selective Probes produce by ThermoFisher scientific, Amax:

550nm, Emax: 570nm). Preparations were then washed in HL3 and analyzed using a Nikon C1 confocal microscope with a 60X water immersion objective.

Mitochondria density analysis

Larvae were dissected as previously described. To quantify mitochondria distribution we compared mitochondrial density in 40µm long proximal and distal regions of the same segmental nerve. Mitochondria density was evaluated by collecting a series of confocal z-stacks to determine the volume of mitochondria (volume of mitoGFP) and the volume of the nerve (volume enclosed by HRP fluorescence). The volume of mitochondria was normalized to the volume of the HRP labeled nerve and the ratio between mitochondria density in distal region and mitochondria density in proximal region was calculated for each nerve.

Image analysis

Confocal images were acquired through x40 or x60 CFI Plan Apochromat Nikon objectives with a Nikon C1 confocal microscope and analyzed using either Nikon EZC1 (version 3.91), Volocity (PaerkinElmer Company, Santa Clara, CA) or NIH ImageJ softwares.

3.4 Biochemical Assays

Mitochondrial Respiration Assay

Oxygen consumption measurements were performed using a Clark type electrode (Hansatech Instruments, King's Lynn, England). Equal weight of larvae were cut up and added to 1 ml of Respiration Buffer (see Appendix A) at room temperature. Total oxygen consumption was calculated by subtracting the rate measured under physiological conditions with that measured after addition of 5 µM Rotenone and 5 µM Antimycin A. Mitochondrial respiration was normalized to total larvae weight.

Activity of respiratory complexes

The redox enzymatic activities were performed on crude mitochondria obtained from third instar larvae of *Drosophila.* Equal weight of larvae was used and frozen in liquid nitrogen and stored at -80°C.

To obtain the crude mitochondria, the larvae were suspended in mitochondrial isolation buffer (70mM sucrose, 200mM Mannitol, 10mM KH_2PO_4, 2mM Hepes, 1mM EGTA, 4mg/ml BSA, pH 7.2) supplemented with protease inhibitors cocktail and homogenized using a glass teflon homogenizer. This and all the subsequent procedures were carried out at 4°C. The homogenate was centrifuged at 600g for 10min in order to precipitate unbroken cells and portions of larvae cuticle. The supernatant was centrifuged again at 10000g for 20min. The mitochondrial pellet was suspended with 200µl of mitochondria isolation buffer and immediately used for analysis.
The enzymatic reactions were performed in constant agitation, at 25°C using a dual wavelength spectrophotometer (V550 Jasco Europe, Italy).

Complex I (NADH-quinone oxidoreductase). The NADH-quinone oxidoreductase activity was assessed following the reduction of 2,6-Dichloro-4-[(4-hydroxyphenyl)imino]-2,5-cyclohexadien-1-one (DCIP) by quinol. After addition of NADH and decylbenzoquionone (DB) in the assay, the reduced quinone (DBH_2) gives electron to the high affinity acceptor DCIP inducing a change color from blue to colorless. The reaction mix is the following:

- Buffer KH^2PO^4 50mM, EDTA 1mM, KCN 2mM, pH 7.6 1 ml
- DCIP 60 µM
- DB 50 µM
- Antimycin A (inhibitor of Complex III) 1 µM
- Crude mitochondria 10 µl

The reaction was started adding 150 µM NADH.
Complex I specific activity was measured at λ= 600nm using a molar extinction coefficient of $19Mm^{-1}cm^{-1}$ for DCIP, after subtraction of 1µM rotenone-insensitive activity.

Complex III (Cytocrome-C oxidoreductase). The enzymatic activity was determined as antimycin A-sensitive ubiquinol: Cytocrome-C reductase activity in the presence of DBH_2. The reaction mix is the following:

- Buffer KH^2PO^4 50mM, EDTA 1mM, KCN 2mM, pH 7.6 1 ml
- $CytC^{3+}$ 20µM
- Rotenone (inhibitor of Complex I) 1µM

- Crude mitochondria 10µl

The reaction was started by adding 50µM DBH_2.

Complex III specific activity was measured at at λ= 550nm using a molar extinction coefficient of 19$Mm^{-1}cm^{-1}$ for Cyt-C^{2+}.

Complex IV (Cytocrome-C oxidase). The enzymatic activity was assessed by the capacity to oxidize Cyt-C^{2+} in Cyt-C^{3+} in presence of oxygen. The reaction mix is the following:

- Buffer KH^2PO^4 50mM, EDTA 1mM, pH 7.6 1 ml
- Cyt-C^{2+} 20µM

The reaction was started by adding 10µl of crude mitochondria.

Complex IV specific activity was measured at λ= 550nm using a molar extinction coefficient of 19$Mm^{-1}cm^{-1}$ for Cyt-C^{2+}.

Citrate Synthase activity. The activity of different ETC enzymes was normalized to Citrate Synthase (CS) activity which is generally considered a mitochondrial mass index[109]. The enzymatic activity was assessed by the ability of CoaSH derived from the reaction to cleave the disulfide bond of DTNB, producing 2-nitro-5-thiobenzoate (TNB^-), which ionizes to the TNB^{2-} dianion in water and has a yellow color.

The reaction mix is the following:

- Buffer TRIS pH8 125mM, 0.1% Tiriton-X 100 0.85 ml
- AcetylCoA (enzyme substrate) 0.3mM
- DTNB 0.1mM
- Crude mitochondria 10µl

After one minute in agitation Oxaloacetic Acid 0.5mM was added to starting the reaction.

CS specific activity was measured at λ= 412nm using a molar extinction coefficient of 13.6 $mM^{-1}cm^{-1}$ for DTNB.

APPENDIX A: Stock and Solutions

LB Medium (Luria-Bertani Medium)

Bacto-tryptone	10g
Yeast extract	5g
NaCl	10g
H_2O	to 1 Liter

Autoclave.

LB Agar

Bacto-tryptone	10g
Yeast extract	5g
NaCl	10g
Agar	20g
H_2O	to 1 Liter

Adjust pH to 7.0 with 5N NaOH. Autoclave.

LB–Ampicillin Agar

Cool 1 Liter of autoclaved LB agar to 55° and then add 100 µg/ml filter-sterilized ampicillin. Pour into petri dishes (~30 ml/100 mm plate).

SOC medium

Bacto-tryptone	20g
Yeast extract	5g
NaCl	0.5g
KCl 1M	2.5 ml
H_2O	to 1 Liter

Adjust pH to 7.0 with 10N NaOH, autoclave to sterilize and add 20 ml of sterile 1M glucose immediately before use.

Drosophila's food

Agar	7 g
Yeast extract	26.4 g
Sucrose	26.4 g
H2O	to 600ml

Autoclave and then add 1.5 g of Nipagin dissolved in 90% ethanol.

Phoshate Buffered Saline (PBS)

KH_2PO_4	15 g/L
NaCl	9 g/L
Na_2HPO_4	8 g/L

Mitochondrial isolation buffer pH 7.2

Sucrose	70 mM
Mannitol	200 mM
KH_2PO_4	10 mM
Hepes	2 mM
EGTA	1 mM
BSA	4 mg/ml

HL3

NaCl	70 mM
KCl	5 mM
CaCl2	1.5 mM
MgCl2	20 mM
NaHCO3	10 mM
Trealosio	5 mM
Sucrosio	115 mM
HEPES	5 mM

Adjust pH to 7.0 with 10N NaOH

Paraformaldeide 4% (PFA)

PFA 8%	10 ml
PBS 5x	4 ml
H_2O	6 ml

Drosophila Genomic DNA extraction solutions

Buffer A	**Buffer B (Store at 4°C)**
100mM tris-HCl pH 7.5	5M Kac
100mM EDTA	6M LiCl
100mM NaCl	
0.5% SDS	

Mowiol 40-88 (Sigma-Aldrich)

Mowiol	2.4 g
Glicerolo	6 g

Shake for 10 min

Add 6 ml of H_2O

Shake for 4h at 50°C.

Add:

Tris/HCl pH 8.5 100 mM	12 ml
DABCO	0.1 %

Centrifuge at 6000 rpm for 15min. Store at -20°C.

TAE 50x

Tris base	242 g
Acetic Acid	57.1 ml
EDTA 0.5 M (pH 8.0)	100 ml
H2O	to 1 Litre

APPENDIX B: Plasmids maps

pBluescript II SK+ (BSSK+)

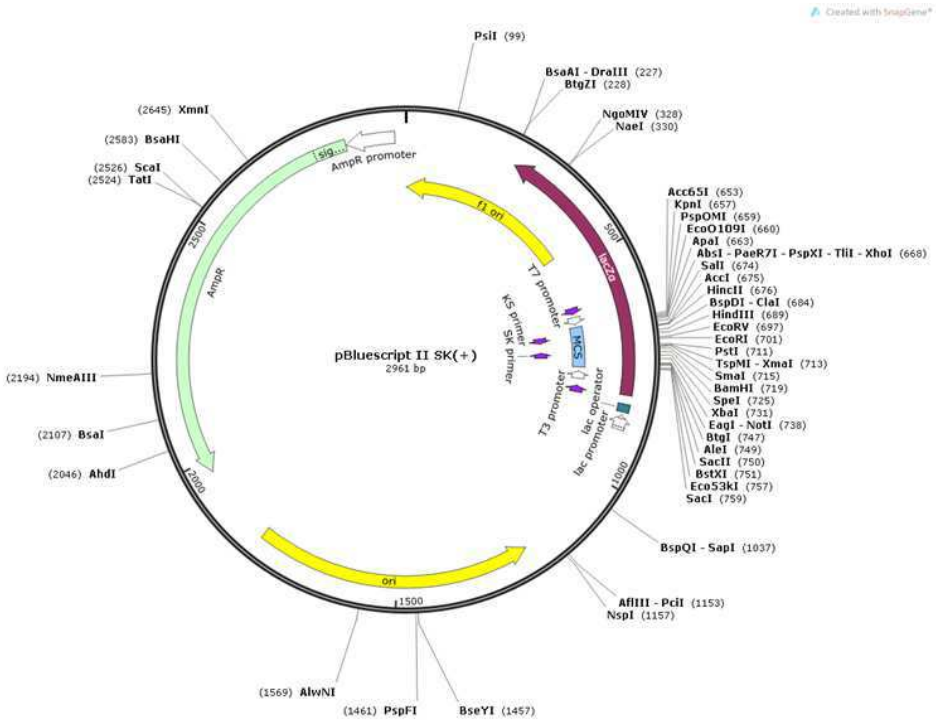

pBS-U6-BbsI-chiRNA

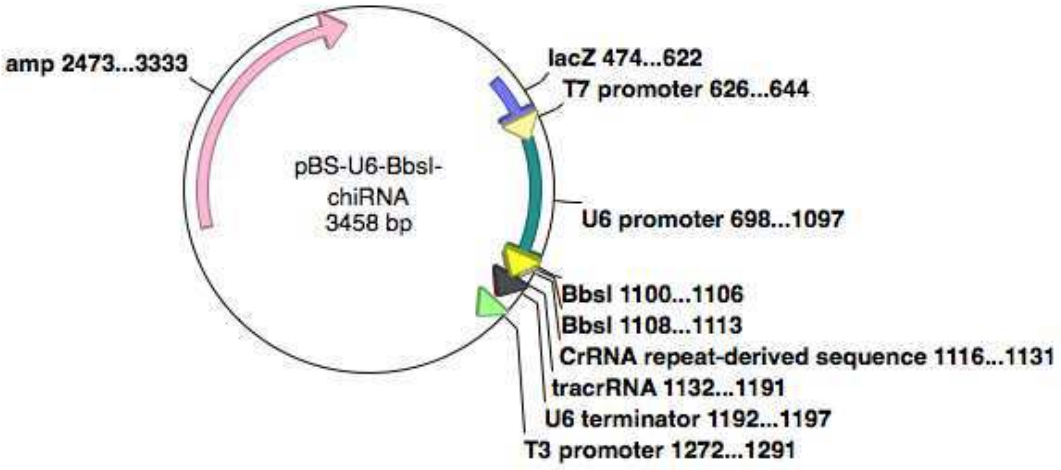

4. RESULTS

4.1 *Drosophila* OPA1 MUTANTS: GENERATION AND PHENOTYPIC CHARACTERIZATION

Generation of mutants

To generate a model of Dominant Optic Atrophy, we introduced disease mutations in the *Drosophila dOPA1* ortholog using the CRISPR/Cas9 system (described previously). Two different *dOPA1* mutants were generated: OPA1 R417H carrying a severe missense mutation and OPA1^{null} which carries a stop codon in position 482 of the dOPA1 protein. Availability of these mutants allowed us to compare the phenotypic effects of a completely null mutation with those induced by the R417H mutations responsible for the DOA plus phenotype in humans.

The experimental design to generate mutants using CRISPR/Cas9 system requires the following steps: (a) generation of the gRNAs responsible for precisely targeting the genomic region where recombination should take place; (b) generation of the dsDNA templates containing the desired genomic modifications to be introduced and homology arms for accurate recombination; (c) choice of a screening method.

(a) To generate the gRNAs we first chose two PAM sites using the online tool FlyCrispr_TargetFinder. The NGG PAM sites have some important features. They should be adjacent or as close as possible to the region of the *dOPA1* gene where the desired mutation is introduced, they must have no potential off-target matches elsewhere in the *Drosophila* genome and they should permit replacement of one of their two Gs by silent mutagenesis such that the fragment introduced by recombination no longer contains a PAM site in that position thereby increasing the efficiency of template incorporation. Figure 12 shows the PAM sites chosen for this project.

AGTCTGATCTGCAGGACCTCCGTCGGGATGTGGAGTTCCGAATGAAGGCGTCGGTGA
GAGGTGGTAAAACCGTCAGCAATGAAGTCATTGCCATGACGGTCAAGGGTCCCGGTC
TGCAACGCATGGTTCTAGTCGATTTGCCAGGAATAATTTCGgtgagcaagtcaatac
aagtaaaactgcgcacatctaatgctaatatcattttagACCATGACTGTCGACATG
GCCTCAGACACAAAAGATTCCATTCACCAGATGACCAAGCATTATATGAGCAATCCG
AACGCCATCATTCTCTGCATTCAGGATGGATCTGTGGACGCTGAGCGCAGTAATGTG
ACAGACTTGGTCATGCAGTGCGATCCCTTGGGTCGACGCACTATTTTTGTGCTCACA
AAGGTGGATCTGGCCGAGGAGCTCGCCGATCCTGATAGAATAAGGAAAATCCTTTCG
GGCAAACTCTTCCCCATGAAGGCTTTGGGCTACTATGCCGTCGTTACCGGTCGTGGA
CGAAAGGATGACAGC

Figure 12: Genomic sequence of portion of the *dOPA1* gene. Green: 5' and 3' PAM sites, the respective target sequences of the gRNA are underlined. Red: c.1250G>A mutation to generate OPA1 *R417H* mutant. Gray: c.1415delT mutation to generate OPA1^{null} mutant.

After choosing the PAM sites targeting gRNAs were completed by adding appropriate genomic targeting sequences. The genomic target sequences should fulfill the following requirements: (1) 20-nt long, (2) followed by a 3-nt PAM sequence **NGG**, (3) begin with a **G** to optimize U6-driven transcription. The resulting sequences of the 5' and 3' gRNA are the following:

5'gRNA: 5'- GGAGTTCCGAATGAAGGCGT**CGG** - 3'

3'gRNA: 5'- GTCATCCTTTCGTCCACGAC**CGG** – 3**'**

Targeting gRNAs were cloned into pU6-BbsI-chiRNA plasmid by annealed oligos via the BbsI restriction sites (Figure 13).

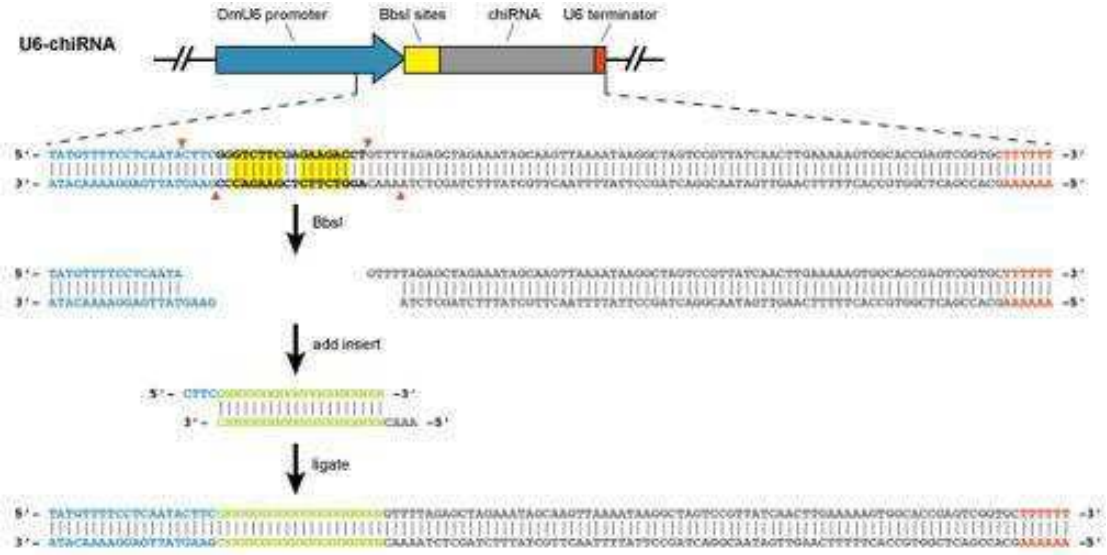

Figure 13: Targeting gRNA: annealing and cloning into pU6-BbsI-chiRNA

(b) To generate the dsDNA templates necessary for homologous recombination we synthesized two DNA fragments each containing the desired disease mutation and the silent mutations required to eliminate the PAM sites present in the wild type genome sequence. (c) In addition to these features, in the synthesized DNA we added a silent mutation that introduces a novel BamHI restriction site necessary for screening the occurrence of homologous recombination events by restriction digest. dsDNA templates also require the presence of two 1500bp homology arms at the 5'-end and 3'-end of the mutated DNA segment that are responsible for homologous pairing during the recombination event. These arms were very simply generated by PCR amplification on genomic *Drosophila* DNA of the two regions adjacent on either side of the DNA fragment to be replaced.

Completion of the dsDNA templates was achieved by assembling the synthesized DNA with the two homology arms. We used a technology known as Gateway assembly cloning where after amplification of each fragment with specific primers containing homologous ends, they were all ligated together in one step into pBluescript II SK+. The following plasmids were produced:

BSSK+OPA1_R417H

BSSK+OPA1^{null}

The vectors BSSK+OPA1_R417H, BSSK+OPA1^{null}, PU6_5'gRNA and 3'gRNA were sent to BestGene Inc. for *Drosophila* embryo injection. The line vas-Cas9-III (BDSC#51324) expressing Cas9 protein in the ovary under control of *vasa* regulatory sequences, was used for microinjection.

Injected embryos were sent to our laboratory where we grew them to adulthood. These adult flies carry the disease mutations in their germ cells, where the Cas9 protein is expressed. Since the *dOPA1* gene is on chromosome II, hatched adults were crossed to a second chromosome balancer stock SM6a/Tft. Hatching adults (F0) were separated by sex. The males were crossed to virgin SM6a/Tft females and the females to SM6a/Tft males. Crosses were performed in vials of standard food. The F1 offspring contained potential mutants. F1 males were then individually crossed to five SM6a/Tft virgins (Figure 14).

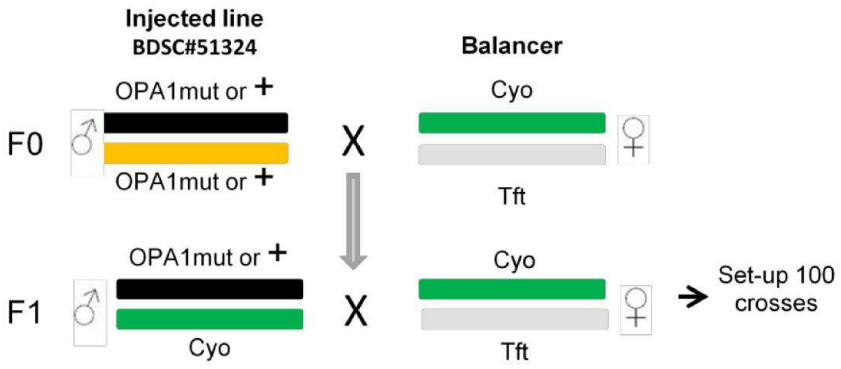

Figure 14: Cross with II chromosome balancer.

About 100 crosses for each construct were set-up and their progeny were screened for the presence of the mutation. Taking advantage of the artificial BamHI site introduced, we performed the screening by PCR followed by restriction digest to identify the mutants.

The size of the amplified PCR fragment is 2719bp. Since The flies tested carry the mutation in heterozygosity we expected that after PCR on genomic DNA, and enzymatic cut with BamHI a positive mutant will show 3 different bands: a 2719bp fragment corresponding to the undigested wt chromosome and 1764bp and 955bp fragments corresponding to the cut mutated chromosome (Figure 15).

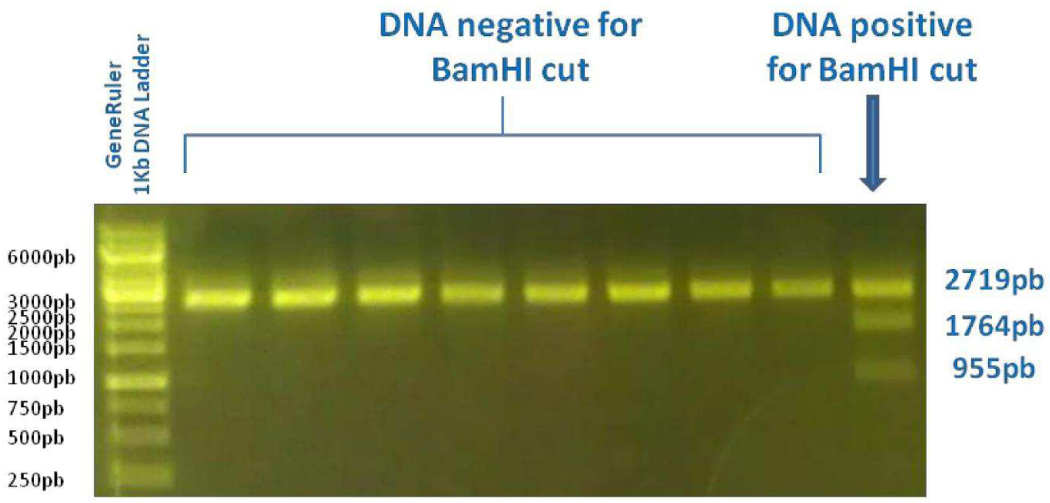

Figure 15: Example of PCR screening. Positive DNA displays three fragments after BamHI digest. The DNA fragments were separated in 1% Agarose gel.

To reduce the time of screening we initially extracted the genomic DNA from a pool of 10 flies, one from each of 10 individual crosses. Once a group of flies turned out positive for BamHI enzymatic cut, the screening was repeated on each individual line of that group. This way we traced back the recombination event to the fly carrying the mutation and. Using this screening method we detected four mutants for every hundred lines analyzed (4% efficiency).

After identifying the mutants the entire portion of recombined genomic DNA was sequenced in order to verify the correct insertion and the presence of all the molecular features artificially introduced (Figure 16).

Mutant OPA1 R417H

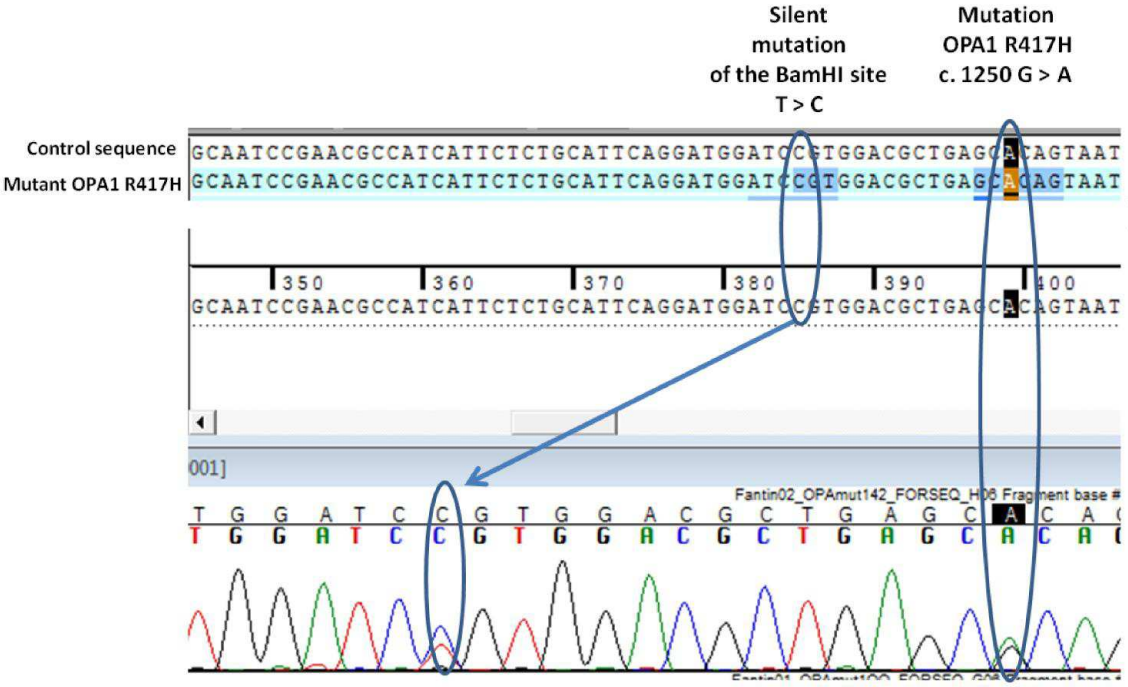

Mutant OPA1^{null}

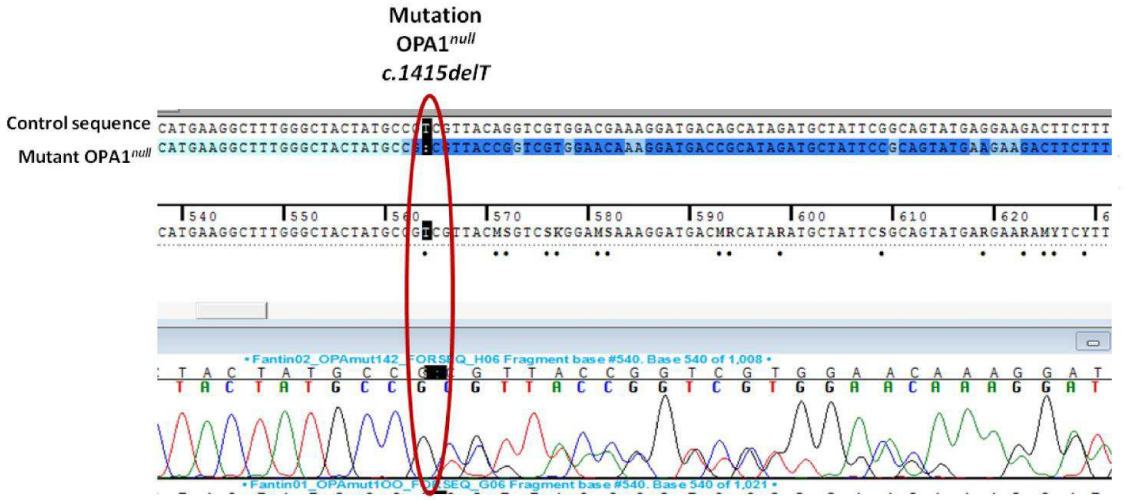

Figure 16: Sequencing of mutants OPA1 R417H and OPA1^{null}.

Phenotypic characterization of CRISPR/Cas9 *dOPA1* mutants

After having verified that the mutants had mutations of interest without any other alterations, the individuals F2 were crossed to each other to generate the stable lines OPA1_R417H/*CyoGFP* and OPA1^{null}/*CyoGFP*. We then initiated a characterization of gross developmental features associated with carrying the generated mutations.

We first checked whether the *dOPA1* mutations were linked to lethality and at what stage lethality occurred. Observations of the adults within the lines shows that both mutations in heterozygosity do not cause any evident morphological alterations. However, both mutations in homozygosity turned out to be lethal. To understand at what developmental stage lethality occurred, we staged the non-fluorescent individuals, i.e. individuals that do not carry the balancer, fluorescent SM6A chromosome and that are therefore homozygous. This analysis showed that R417H homozygous mutants develop until the second instar larva stage whereas the OPA1^{null} homozygotes die earlier at the first instar larva stage (Figure 17).

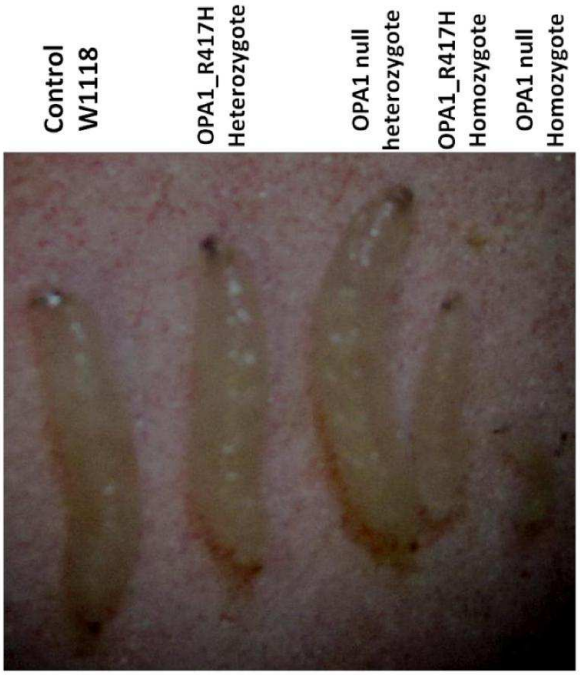

Figure 17: Comparison of control W1118, OPA1 R417H heterozygote, OPA1^{null} heterozygote, OPA1R417H homozygote and OPA1^{null} homozygote larvae.

This observation shows that the OPA1 R417H mutation is slightly less severe than OPA1^{null} suggesting that it causes an important but partial inactivation of the protein function. However we were more interested in studying the heterozygote *dOPA1* mutants because DOA is a dominant disease. To check if the heterozygous mutations have effects on flies, we performed a longevity assay on a large cohort (n=600/genotype) of control W^{1118}, OPA1 R417H and OPA1^{null}. *Drosophila* were maintained at 18°C at 40-50 flies/vial and were transferred to fresh food and counted every 3 days.

As shown in Figure 16, the mutants strains display a robust reduction in lifespan. In controls 50% of survival is reached at 47 days, in OPA1^{null} and OPA1 R417H mutants this parameter goes down to 28 and 24 days respectively. No obvious differences between the two mutants were detectable using our assay.

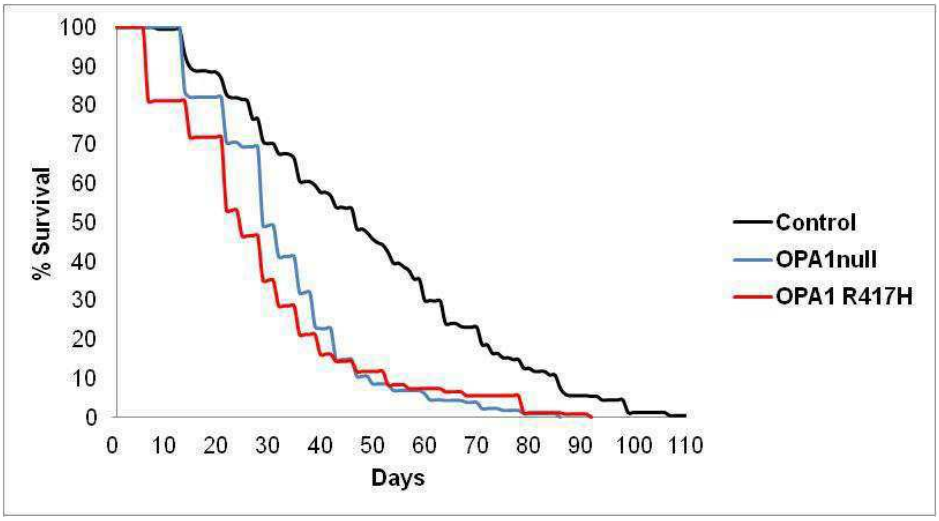

Figure 18: Heterozygous *dOPA1* mutation shortens lifespan in *Drosophila.*

The lifespan reduction of both *dOPA1* mutants indicate that the heterozygous mutations of OPA1 is likely to cause systemic consequences probably affecting multiple processes. This dominant effect on lifespan is interesting in consideration of the fact that OPA1 pathology is also dominant and suggests that these flies can potentially offer a useful disease model.

4.2 ANALYSIS OF MITOCHONDRIAL DYNAMICS

It is known that the OPA1 protein is involved in mitochondrial dynamics, the literature suggests that in DOA patients the mitochondrial network is altered in different tissues, therefore we performed a series of experiments to analyze mitochondrial morphology in the neuronal and muscular systems of both *dOPA1* mutants.

Mitochondrial morphology and distribution in *Drosophila* larvae nerves

To evaluate the state of mitochondrial dynamics in the nervous system we analyzed mitochondrial morphology within the nerves of *Drosophila* third instar larvae.

Control W^{1118}, OPA1 R417H and $OPA1^{null}$ heterozygote mutants were crossed to ELAV-Gal4,UAS-mitoGFP/TM6 line in order to fluorescently label neuronal mitochondria (Figure 19a).

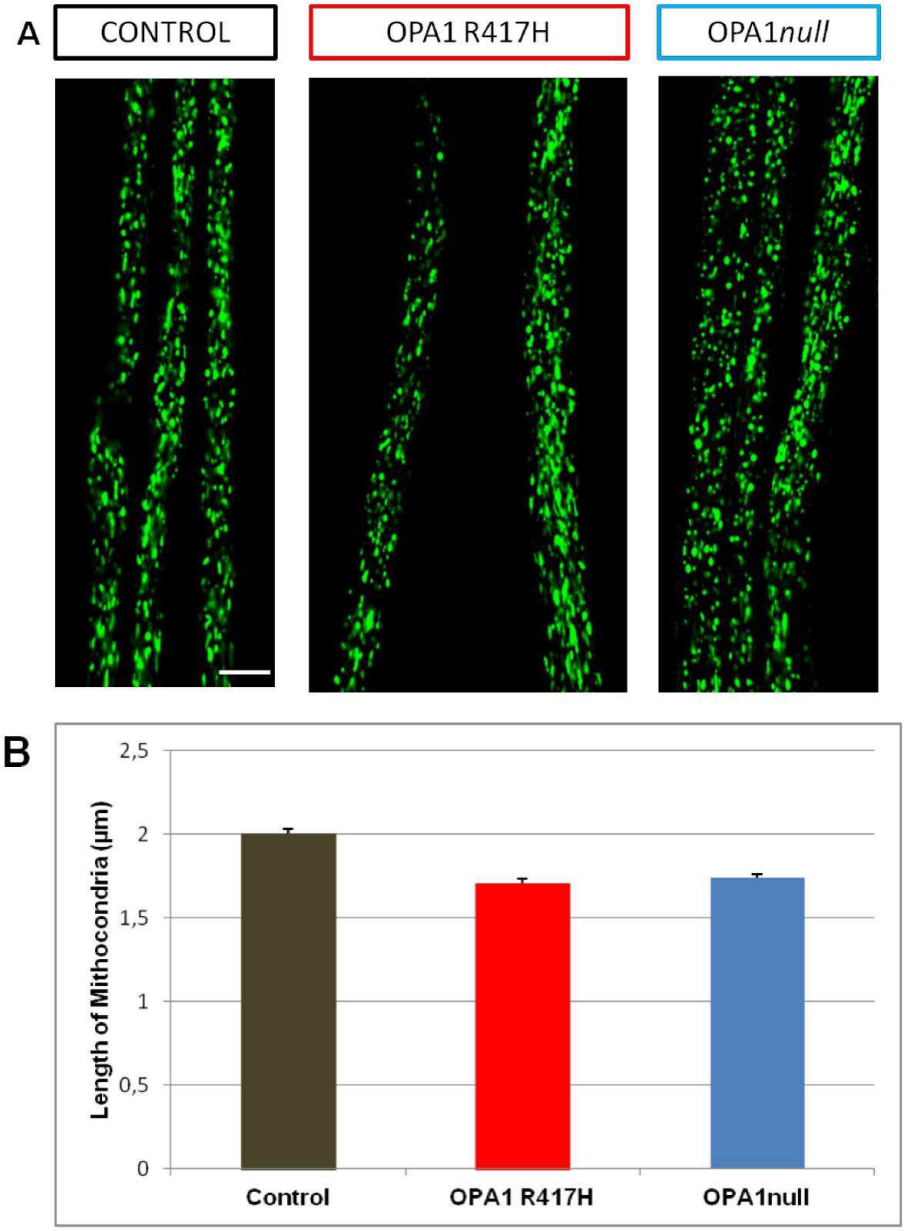

Figure 19: Mitochondria morphology in nerves of *Drosophila*. Control W^{1118} and *dOPA1* mutants were crossed to the pan-neuronal drivers ELAV-Gal4 and UAS-mitoGFP to label neuronal mitochondria. (**A**) Confocal images of third instar larva nerves. Scale bar 10µm. **(B)** Analysis of the mitochondrial length in nerves. For each genotype 10 images of nerves were analyzed with Volocity. n(larvae) >3. Error bars represent SEM.

As shown in figure 19a, mitochondrial fragmentation is not evident at first sight. However, analysis of the length of individual fluorescent spots with a specific software reveals that a reduction of the average length of mitochondria was detectable in *dOPA1* mutants when compared to controls (Figure 19b). This result indicates that mitochondria morphology is affected by mutation of a single copy of the fly dOPA1 gene.

Existing evidence intimates that dysfunction of the mitochondrial dynamics alters mitochondrial axonal distribution. We thus went on to investigate the distribution of mitochondria in segmental nerves of *Drosophila* third instar larvae. Mitochondria were labeled in control and *dOPA1* mutants using mitoGFP expressed under the control of the D42-gal4 driver line which specifically expresses specifically in motor neurons thus labeling the larva segmental nerves. were crossed to UAS-mitoGFP,D42-Gal4/TM6. The nerves where identified by simultaneous labeling of axonal membranes using the neuronal marker HRP. Mitochondria distribution along the nerves was then evaluated by measuring mitochondrial density in proximal (250 μm away from the cell bodies) and distal (1500 μm away from the cell bodies) regions of the segmental nerves.

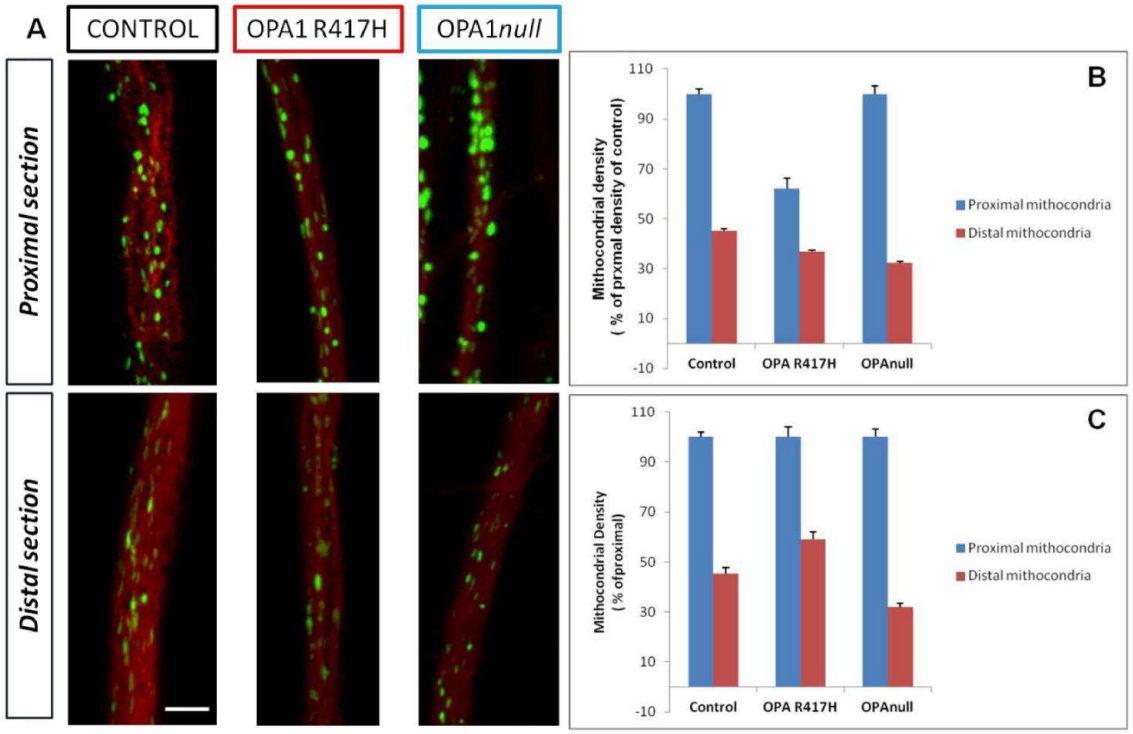

Figure 20: Mitochondria distribution in axons of motoneurons. Control W^{1118} and *dOPA1 mutants* were crossed to motoneuronal driver D42-Gal4 and UAS-mitoGFP to label mitochondria. **(A)** Confocal images of third instar larva segmental nerves. For each genotype a proximal (A2) and a distal (A5) section of the same nerve are shown. Scale bar 5µm. **(B)** The bar graph show for each experimental genotype the proximal and distal mitochondria density normalized to the proximal density of controls. **(C)** The graph shows mitochondria density in the distal region of each genotype normalized to its corresponding proximal region. Error bar represent SEM. n=10, n (larvae)> 3.

In OPA1 R417H heterozygotes we found a general reduction of mitochondria density both proximally and distally compared to controls, whereas in $OPA1^{null}$ heterozygote mutants the reduction of mitochondrial density was present only in distal nerve segments (Figure 20b). Mitochondrial density in the distal region of control nerves was reduced to 45% of the density in the proximal region indicating that a progressive loss of density is normal in long axons. However, this physiological decrease in density was enhanced in $OPA1^{null}$ mutants but not in OPA1 R417H (Figure 20c). In fact in OPA1 R417H mutant there is a more generalized reduction whereas in $OPA1^{null}$ mutants the ability of mitochondria to move and distribute along the axons appears to be affected. These data suggest that the two *dOPA1* mutations lead to reduction of mitochondria in long axons through different mechanisms.

Mitochondrial morphology in *Drosophila* larvae muscles

To assess mitochondrial morphology in muscles of *dOPA1* mutants, we performed confocal microscopy on *Drosophila* larvae. To verify that indeed mutation of dOPA1 causes mitochondria morphology defects in muscles we first examined the mitochondria network in body wall muscles of third instar larvae homozygous for both the dOPA1 mutations we generated. Because in the homozygous background we were unable to express mito-GFP and thus unable to visualize the mitochondria, we resorted to using the mitochondrion-selective probe as MitoTracker red. Labeling can be performed on living, dissected larvae because unlike neuronal membranes that are essentially not permeable to MitoTracker, muscles are nicely labeled by this dye in vivo. Therefore, homozygous larvae of both *dOPA1* mutants and control W^{1118} were dissected and observed in live-confocal microscopy after labeling with MitoTraker-red (figure 21).

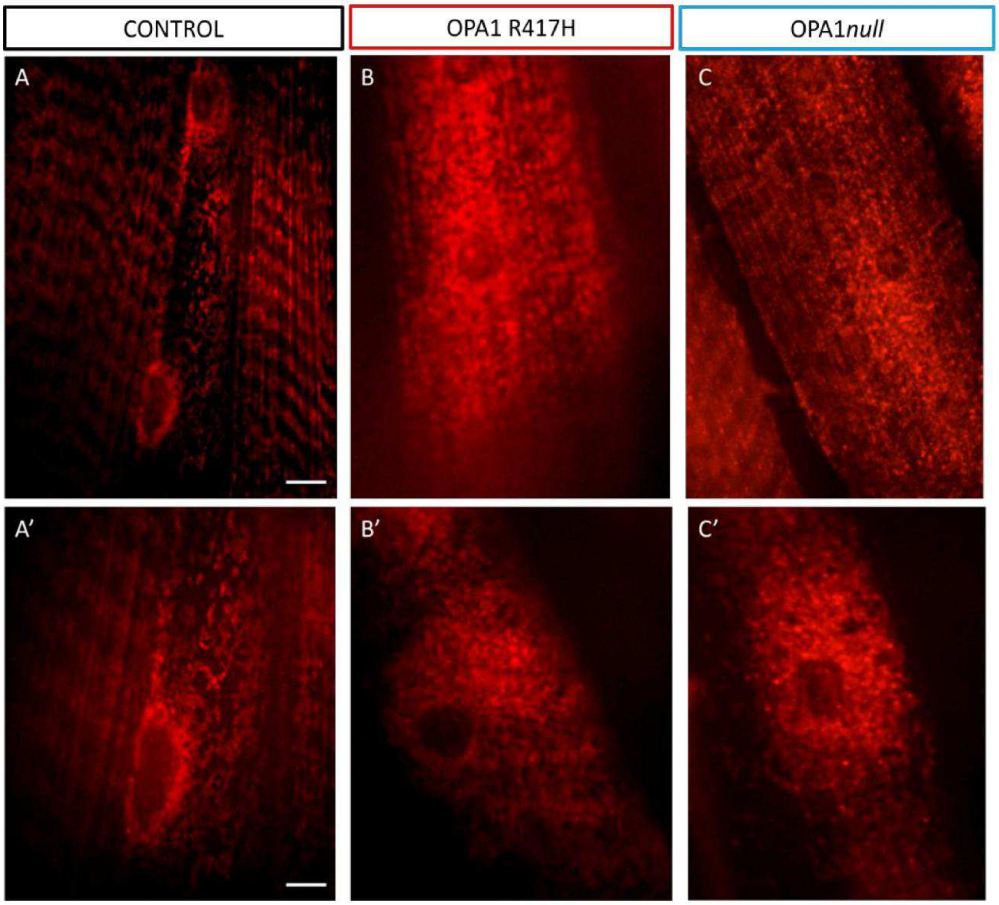

Figure 21: Mitochondria morphology in muscles of homozygose mutants and control larvae. Representative of live-confocal images of body wall muscles in Control W^{1118},OPA1 R4174H homozygote and $OPA1^{null}$ homozygote labeling using MitoTraker-red. A,B,C Scale bar 15µm. A',B'.C' Scale bar 5 µm.

Analysis of mitochondrial morphology in larval muscles confirmed the importance of the OPA1 protein in controlling mitochondrial network shape, since both R417H and the null *dOPA1* mutations produce an obvious alteration of the mitochondria network in larval muscles. In fact, figure 21 shows that the nice sarcomeric pattern present in control muscles is lost in both mutants which are characterized also by marked clumping and clustering.

To create a useful pathology model however, we need to examine the defects associated with dominant effects of the mutations. To this end we took advantage of the UAS-mito-GFP transgenic line to more easily label mitochondria. Control W^{1118}, OPA1 R417H and $OPA1^{null}$ lines were crossed to UAS-mitoGFP,mef2-Gal4/TM6, a recombinant line that expresses mitoGFP specifically in muscle mitochondria. We examined third instar larva body wall muscles in both heterozygote mutants. As shown in figure 22, in control third instar larvae muscle mitochondria are abundantly distributed along the length of the myofibers revealing a nice sarcomeric pattern, whereas both *dOPA1* mutants display slightly altered mitochondrial architecture and distribution, with some clusterization of the organelles in the perinuclear region indicating that mutation of *dOPA1* affects dominantly mitochondrial morphology.

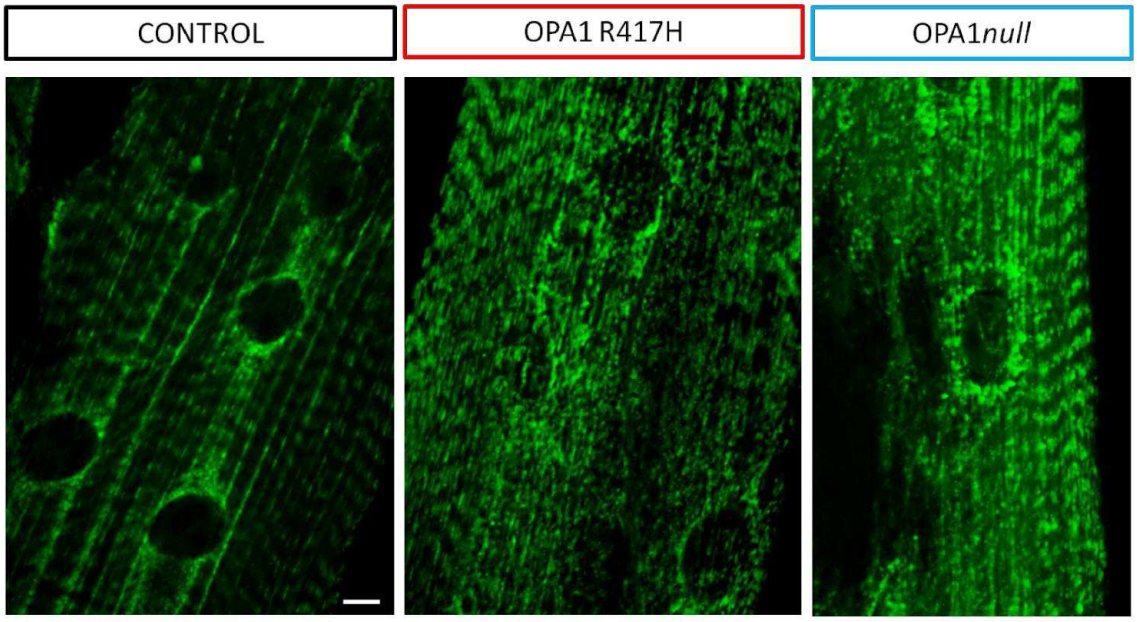

Figure 22: Mitochondria morphology in muscles of third instar larvae. Representative confocal images of body wall muscles in Control (+/+;UAS-mitoGFP,mef2-Gal4/+), OPA1 R4174H heterozygote (OPA1R417H/+; UAS-mitoGFP,mef2-Gal4/+), $OPA1^{null}$ heterozygote ($OPA1^{null}$/+; UAS-mitoGFP,mef2-Gal4/+). Scale bar 15µm.

4.3 Analysis of the mitochondria functions

Because perturbation of the activity of mitochondrial dynamics is known to affect also mitochondria function, we hypothesized that an impairment of mitochondrial function might be responsible for the observed reduction of lifespan in *dOPA1* mutants . To test this hypothesis in our fly models, we performed functional assays aimed at establishing whether mitochondria respiration was affected.

Mitochondrial respiration in Drosophila larvae homogenate

The different complexes of respiratory chain are located in the inner mitochondrial membrane, mutations of a inner mitochondrial membrane proteins as OPA1 results of reduction of this parameter. In order to evaluate oxygen consumption in *dOPA1* mutants, a respiration assay was performed using a Clark type electrode on total larvae homogenate of: control W^{1118}, heterozygous and homozygous OPA1 R417H, heterozygous and homozygous $OPA1^{null}$ individuals (Figure 23).

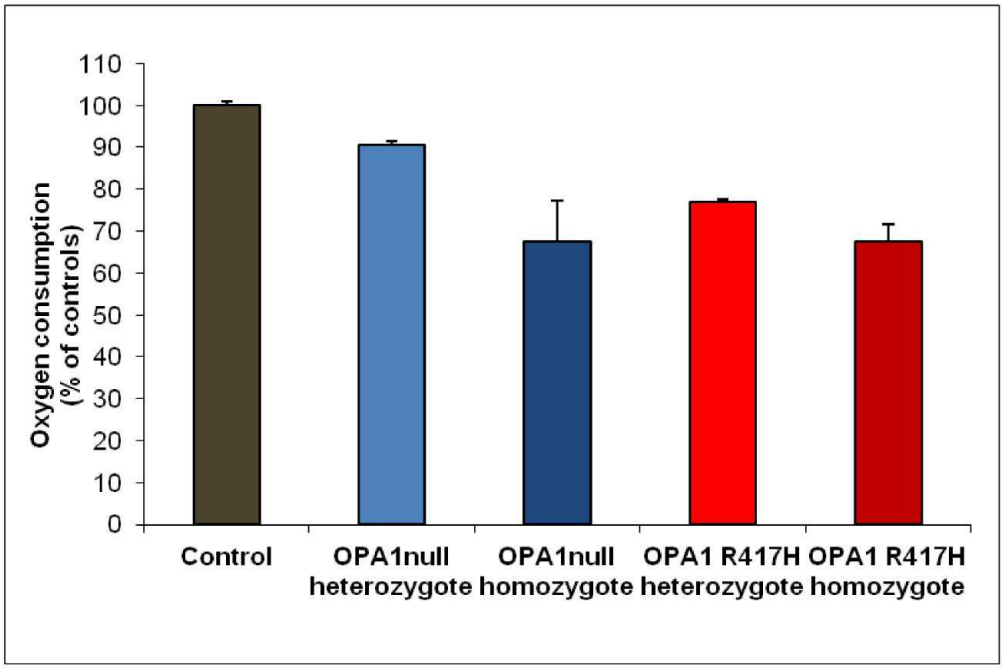

Figure 23: Mitochondria respiration assay. *Drosophila* larvae were homogenate, control W^{1118} -10 larvae, $OPA1^{null}$ heterozygote- 40 larvae, $OPA1^{null}$ homozygote - 60 larvae, OPA1 R417H heterozygote – 40 larvae, OPA1 R417H homozygote- 60 larvae. Basal oxygen consumption was normalized to tissue weight. Data represent the mean of three independent experiments and error bars indicate SEM. $P<0.01$.

Analysis of mitochondrial respiratory capacity shows that in larvae homozygous for *dOPA1* mutations oxygen consumption was reduced by approximately 35% compared to controls; whereas in heterozygous larvae OPA1^{null} and OPA1 R417H , oxygen consumption was reduced by 20% and 10% respectively of that of controls (Figure 23).

These data indicate that mutations on *dOPA1* protein with morphological alterations of mitochondria shape cause reduction of the mitochondrial functions. Although this was an expected result based on the available literature, it is interesting to underscore the observation that the OPA1 R417H mutation in heterozygosity causes a greater reduction of mitochondrial respiration compared to an heterozygote OPA1^{null} mutant.

Analysis of the activity of respiratory complexes

In order to confirm the results observed on mitochondrial respiration, the redox activity of respiratory complexes was measured in a spectrometry assay using crude mitochondria extracted from third instar larvae of control W^{1118}, heterozygous and homozygous OPA1 R417H, heterozygous and homozygous OPA1^{null} individuals. The activities of complex I (CI), complex III (CIII) and complex IV (CIV) were normalized to Citrate Synthase (CS) activity. CS activity is universally accepted as an index of mitochondrial mass since it is encoded in the nucleus and localized in the mitochondrial matrix.

The bar graph in figure 24 shows the redox activity of different ETC complexes. CI activity was reduced in both homozygous *dOPA1* mutants, especially in OPA1^{null} homozygote mutant, as well as in heterozygous OPA1 R417H. Surprisingly, CI activity of OPA1^{null} heterozygotes was similar to controls, suggesting that the mutated copy of OPA1 R417H alters CI activity more than a reduced expression of OPA1. Furthermore, also complex IV activity was strongly affected in OPA1 R417H heterozygote and slightly reduced in the other mutants. Finally, CIII activity resulted similar to controls or enhanced in OPA1^{null} heterozygotes.

These data confirm that mutation of *dOPA1* causes a reduction of mitochondrial function. The most interesting result concerns the heterozygous mutant OPA1 R417H in which the activities of CI and CIV are drastically reduced. Again, this result suggests that some functional parameters are more severely altered by

the presence of a single copy of a severe pathological mutation than by the presence of a single copy of a complete loss of function allele.

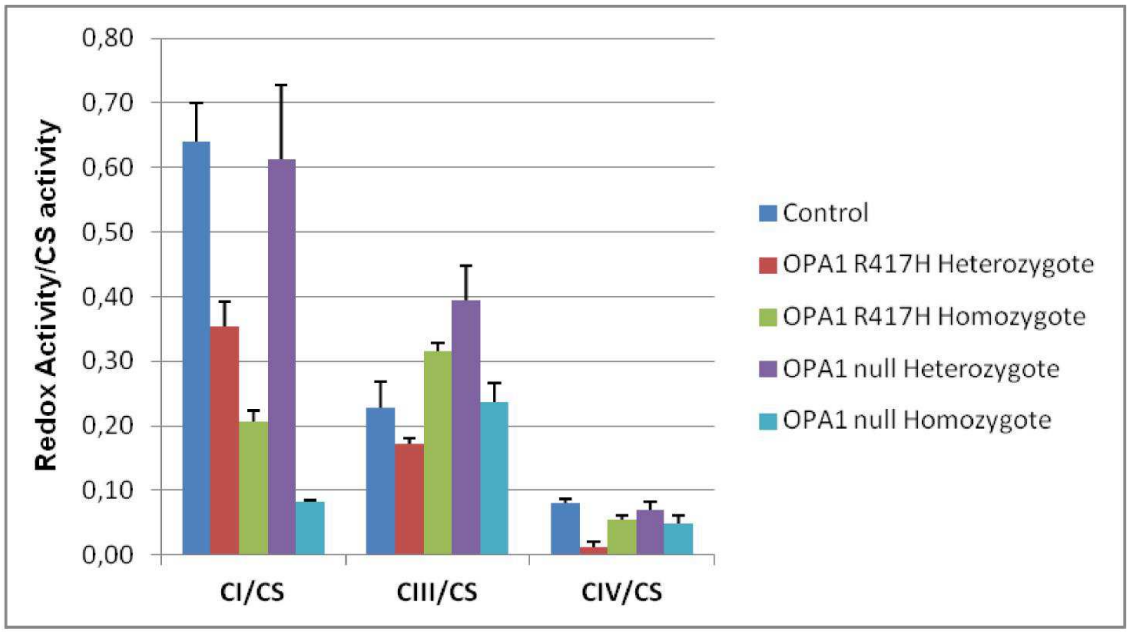

Figure 24: Respiratory complex activity. CI (NADH:DB:DCIP), CIII (DBH2:cytochrome c), CIV (reduced cytochrome c:O2), activities were determined as described in the methods section. Data represent the mean of three independent measurements and error bars indicate SD.

5. DISCUSSION

The mechanisms by which OPA1 mutations produce DOA or DOA plus in humans are not clear. A broad mutational spectrum has been observed for OPA1 mutations. Over 250 *OPA1* mutations have so far been reported and they can be grouped into two main categories depending on whether they are predicted to cause disease due to haploinsufficiency (deletions, insertions, splice site and nonsense mutations) or can potentially act through a dominant-negative mechanism (missense mutations)[68]. Although optic atrophy is the defining feature of DOA, a specific missense mutation within the *OPA1*gene, R455H, has been consistently associated with a number of additional clinical manifestations including sensorineural deafness, chronic progressive external ophthalmoplegia ataxia, myopathy and peripheral neuropathy thus giving rise to the so called DOA plus phenotype.

To address the pathophysiological mechanism of OPA1 mutations we have taken advantage of the outstanding sequence homology between the human and Drosophila OPA1 (*dOPA1*) proteins has allowed us to use *Drosophila* as model system to attempt an investigation of the mode of action of different categories of OPA1 mutations, a nonsense mutation predicted to be haploinsufficient and a missense mutation R417H homologous to human R445H, thought to exert a dominant negative effect. Because the R455H mutation has been linked to a DOA plus phenotype, it is believed to be a more severe mutation, at least in a heterozygous state, than a null. To model these mutations we have used the latest genome engineering technology, in vivo CRISPR/Cas9 to modify the endogenous *Drosophila* OPA1 gene. To our knowledge this is the first reported instance of a model organism that carries a systemic pathogenic OPA1 mutation. Comparison of the two *dOPA1* mutants generated has allowed an initial assessment of the phenotypes elicited by the mutations fundamentally revealing that two types of mutations show a number of differences in their in vivo behavior. The first important observation concerns viability. Since we are dealing with a fully mutant organism we have been able to examine the effects of the mutations on viability. Not surprisingly, we found that both mutants are lethal in homozygosity thus underscoring the importance of OPA1 function for the organism. However, lethality occurs at a different

developmental stage. Homozygous null mutants (carrying the nonsense mutation) die at the first instar larva stage while homozygous R417H mutants die later, around the second instar larva stage. This result shows that not having the OPA1 protein at all turns out to be a more severe condition than having a R417H mutant OPA1 under this paradigm. However, both DOA and DOA plus are dominant diseases and therefore caused by mutation of a single copy of the gene in the heterozygous state[66]. Examination of both heterozygous *Drosophila* mutants shows that they are viable but revealed also that they display a similar shortening of lifespan, suggesting that under an heterozygosity paradigm they behave similarly. However, the presence of more subtle differences in lifespan may be hindered by the rather gross experimental approach. Confirmation of the observation that heterozygous *dOPA1* mutants display defects has come from the analysis of mitochondria morphology which has shown that both in nerves and muscles mitochondria network shape is characterized by mild fragmentation and clusterization. Yet, it remains absolutely clear that a single copy mutation of the OPA1 gene in flies displays a dominant effect likely due to perturbation of mitochondria morphology which in turn causes systemic defects that result in shortened lifespan. This is reminiscent of the condition in humans where onset of DOA or DOA plus disease demonstrates that alteration of a single copy of OPA1 has harmful consequences for the organism.

How does perturbation of mitochondria morphology lead to the dominant systemic consequences observed in our *dOPA1* mutants? It has been reported that loss or mutation of OPA1 is associated with impairment of oxidative phosphorylation. In agreement with these reports, we found that both homozygous mutants display a substantial decrease in oxygen consumption. However, it is interesting to note that despite a similar effect on mitochondrial morphology the null mutation and the R417 mutation behaved differently in the respiration assay. Indeed, the observation that R417 heterozygote individual show a greater decrease of oxygen consumption when compared to null heterozygotes seem to suggest that that some functional parameters are more severely altered by the presence of a single copy of a missense pathological mutation than by the presence of a single copy complete loss of function allele. This result appears to be in line with the fact that R417H has been linked to

DOA plus, a more severe pathology than DOA which is normally associated with OPA1 haploinsufficiency[66, 68, 110]. This would indicate that also in an organism model R417H may lead to a dominant interfering effect on the wild type OPA1 protein thus accounting for the greater severity of the R417H mutation compared to the null mutation. Therefore, the Drosophila models we have generated appear to reproduce to some extent features that are typical of OPA1 affected individuals. A previous report[111] has shown that in fibroblasts derived from patients carrying a R445H mutation (homologous to the R417H fly mutant) the rate of mitochondria ATP synthesis was significantly decreased at the level of complex I thus pointing to complex I as the culprit for the defective oxidative phosphorylation. Although we also found that the activity of complex I was generally reduced for both *dOPA1* null and R417H homozygous mutants, it was surprisingly normal in *dOPA1* null heterozygous individuals while it was reduced to about 50% of controls in R417H heterozygous individuals. Even more striking are the results regarding complex IV activity since essentially both homozygous mutants as well as the *dOPA1* null heterozygote are unaffected. Unexpectedly, however, complex IV activity was largely diminished in *dOPA1* R417H heterozygous individuals. These results further point to a different behavior for the two mutations in vivo in a whole organism, with the DOA plus causing mutation R417H leading to more severe effects than the nonsense, null mutation.

In this thesis work we have investigated the role of two types of pathogenic mutations in the endogenous OPA1 gene using *Drosophila* as a model system. One mutation completely obliterates OPA1 function and has been linked in humans to DOA pathology through a haploinsufficient mechanism. The other type is a severe missense mutation whose occurrence in humans is thought to give rise to the more severe DOA plus pathology by functioning as a dominant negative allelic form. Our novel animal models appear to suggest that indeed the two types of mutation differentially affect some of the morphological and functional parameters of mitochondria when heterozygous. We have observed that in none of the experiments conducted the null heterozygous mutation had worse consequences than the R417H mutation. It either behaved the same way or was obviously milder. This result is in apparent contrast with the observation that in homozygosity the null mutant dies at a very early developmental stage

while the R417H homozygote carries on until a later stage but can be explained by viewing the R417H as a partially though severely inactivating mutation and thus by definition weaker than a completely inactivating one. However, in heterozygosity R417H could interfere with the activity of the wild type copy of *dOPA1* resulting in more severe phenotypes than those caused by the presence of a single loss of function allele. Furthermore, the fact that some tests do not show differences between the two mutations can easily be ascribed to the coarseness of the test itself that would not permit to discriminate relatively subtle divergences.

We believe that we have produced a rather good model to study the etiopathology of different forms of DOA caused by different classes of mutations within the OPA1 gene. Further validation of these models is obviously still required and is already under way.

6. Reference

1. Westermann, B. Mitochondrial fusion and fission in cell life and death. *Nat. Rev. Mol. Cell Biol.* **11**, 872-884 (2010).

2. Burté, F., Carelli, V., Chinnery, P. F. & Yu-Wai-Man, P. Disturbed mitochondrial dynamics and neurodegenerative disorders. *Nat. Rev. Neurol.* **11**, 11-24 (2015).

3. Nisoli, E. & Carruba, M. O. Nitric oxide and mitochondrial biogenesis. *J. Cell. Sci.* **119**, 2855-2862 (2006).

4. Hales, K. G. & Fuller, M. T. Developmentally Regulated Mitochondrial Fusion Mediated by a Conserved, Novel, Predicted GTPase. *Cell* **90**, 121-129 (1997).

5. Fritz, S., Rapaport, D., Klanner, E., Neupert, W. & Westermann, B. Connection of the mitochondrial outer and inner membranes by Fzo1 is critical for organellar fusion. *J. Cell Biol.* **152**, 683-692 (2001).

6. Rojo, M., Legros, F., Chateau, D. & Lombès, A. Membrane topology and mitochondrial targeting of mitofusins, ubiquitous mammalian homologs of the transmembrane GTPase Fzo. *J. Cell. Sci.* **115**, 1663-1674 (2002).

7. Meeusen, S. *et al*. Mitochondrial Inner-Membrane Fusion and Crista Maintenance Requires the Dynamin-Related GTPase Mgm1. *Cell* **127**, 383-395 (2006).

8. McQuibban, G. A., Saurya, S. & Freeman, M. Mitochondrial membrane remodelling regulated by a conserved rhomboid protease. *Nature* **423**, 537-541 (2003).

9. Cipolat, S., De Brito, O. M., Dal Zilio, B. & Scorrano, L. OPA1 requires mitofusin 1 to promote mitochondrial fusion. *Proc. Natl. Acad. Sci. U. S. A.* **101**, 15927-15932 (2004).

10. Yarosh, W. *et al*. The molecular mechanisms of OPA1-mediated optic atrophy in Drosophila model and prospects for antioxidant treatment. *PLoS Genet.* **4**, 0062-0071 (2008).

11. Koshiba, T. *et al*. Structural basis of mitochondrial tethering by mitofusin complexes. *Science* **305**, 858-862 (2004).

12. DeVay, R. M. *et al*. Coassembly of Mgm1 isoforms requires cardiolipin and mediates mitochondrial inner membrane fusion. *J. Cell Biol.* **186**, 793-803 (2009).

13. Smirnova, E., Shurland, D. -., Ryazantsev, S. N. & Van Der Bliek, A. M. A human dynamin-related protein controls the distribution of mitochondria. *J. Cell Biol.* **143**, 351-358 (1998).

14. Mozdy, A. D., McCaffery, J. M. & Shaw, J. M. Dnm1p GTPase-mediated mitochondrial fission is a multi-step process requiring the novel integral membrane component Fis1p. *J. Cell Biol.* **151**, 367-379 (2000).

15. Zhang, Y. & Chan, D. C. Structural basis for recruitment of mitochondrial fission complexes by Fis1. *Proc. Natl. Acad. Sci. U. S. A.* **104**, 18526-18530 (2007).

16. Tieu, Q., Okreglak, V., Naylor, K. & Nunnari, J. The WD repeat protein, Mdv1p, functions as a molecular adaptor by interacting with Dnm1p and Fis1p during mitochondrial fission. *J. Cell Biol.* **158**, 445-452 (2002).

17. Lackner, L. L., Horner, J. S. & Nunnari, J. Mechanistic analysis of a dynamin effector. *Science* **325**, 874-877 (2009).

18. Ingerman, E. *et al*. Dnm1 forms spirals that are structurally tailored to fit mitochondria. *J. Cell Biol.* **170**, 1021-1027 (2005).

19. James, D. I., Parone, P. A., Mattenberger, Y. & Martinou, J. -. hFis1, a novel component of the mammalian mitochondrial fission machinery. *J. Biol. Chem.* **278**, 36373-36379 (2003).

20. Yoon, Y., Krueger, E. W., Oswald, B. J. & McNiven, M. A. The mitochondrial protein hFis1 regulates mitochondrial fission in mammalian cells through an interaction with the dynamin-like protein DLP1. *Mol. Cell. Biol.* **23**, 5409-5420 (2003).

21. Lee, Y. -., Jeong, S. -., Karbowski, M., Smith, C. L. & Youle, R. J. Roles of the mammalian mitochondrial fission and fusion mediators Fis1, Drp1, Opa1 in apoptosis. *Mol. Biol. Cell* **15**, 5001-5011 (2004).

22. Breckenridge, D. G. *et al*. Caenorhabditis elegans drp-1 and fis-2 Regulate Distinct Cell-Death Execution Pathways Downstream of ced-3 and Independent of ced-9. *Mol. Cell* **31**, 586-597 (2008).

23. Gandre-Babbe, S. & Van Der Bliek, A. M. The novel tail-anchored membrane protein Mff controls mitochondrial and peroxisomal fission in mammalian cells. *Mol. Biol. Cell* **19**, 2402-2412 (2008).

24. Merz, S. & Westermann, B. Genome-wide deletion mutant analysis reveals genes required for respiratory growth, mitochondrial genome maintenance and mitochondrial protein synthesis in Saccharomyces cerevisiae. *Genome Biol.* **10** (2009).

25. Chen, H., McCaffery, J. M. & Chan, D. C. Mitochondrial Fusion Protects against Neurodegeneration in the Cerebellum. *Cell* **130**, 548-562 (2007).

26. Li, Z., Okamoto, K., Hayashi, Y. & Sheng, M. The Importance of Dendritic Mitochondria in the Morphogenesis and Plasticity of Spines and Synapses. *Cell* **119**, 873-887 (2004).

27. Amchenkova, A. A., Bakeeva, L. E., Chentsov, Y. S., Skulachev, V. P. & Zorov, D. B. Coupling membranes as energy-transmitting cables. I. Filamentous mitochrondia in fibroblasts and mitochondrial clusters in cardiomyocytes. *J. Cell Biol.* **107**, 481-495 (1988).

28. Balaban, R. S., Nemoto, S. & Finkel, T. Mitochondria, Oxidants, and Aging. *Cell* **120**, 483-495 (2005).

29. Nakada, K. *et al*. Inter-mitochondrial complementation: Mitochondria-specific system preventing mice from expression of disease phenotypes by mutant mtDNA. *Nat. Med.* **7**, 934-940 (2001).

30. He, C. & Klionsky, D. J. Regulation mechanisms and signaling pathways of autophagy. *Annu. Rev. Genet.* **43**, 67-93 (2009).

31. Twig, G. *et al*. Fission and selective fusion govern mitochondrial segregation and elimination by autophagy. *EMBO J.* **27**, 433-446 (2008).

32. Youle, R. J. & Karbowski, M. Mitochondrial fission in apoptosis. *Nat. Rev. Mol. Cell Biol.* **6**, 657-663 (2005).

33. Suen, D. -., Norris, K. L. & Youle, R. J. Mitochondrial dynamics and apoptosis. *Genes Dev.* **22**, 1577-1590 (2008).

34. Fannjiang, Y. *et al*. Mitochondrial fission proteins regulate programmed cell death in yeast. *Genes Dev.* **18**, 2785-2797 (2004).

35. Goyal, G., Fell, B., Sarin, A., Youle, R. J. & Sriram, V. Role of Mitochondrial Remodeling in Programmed Cell Death in Drosophila melanogaster. *Developmental Cell* **12**, 807-816 (2007).

36. Jagasia, R., Grote, P., Westermann, B. & Conradt, B. DRP-1-mediated mitochondrial fragmentation during EGL-1-induced cell death in C. elegans. *Nature* **433**, 754-760 (2005).

37. Frank, S. *et al*. The Role of Dynamin-Related Protein 1, a Mediator of Mitochondrial Fission, in Apoptosis. *Developmental Cell* **1**, 515-525 (2001).

38. Poos, G. I. *et al*. Structure-activity studies with the selective rat toxicant norbormide. *J. Med. Chem.* **9**, 537-540 (1966).

39. Rennison, D. *et al*. Synthesis and activity studies of analogues of the rat selective toxicant norbormide. *Bioorg. Med. Chem.* **15**, 2963-2974 (2007).

40. Ricchelli, F. *et al*. Species-specific modulation of the mitochondrial permeability transition by norbormide. *Biochim. Biophys. Acta* **1708**, 178-186 (2005).

41. Zulian, A. *et al*. Assessing the molecular basis for rat-selective induction of the mitochondrial permeability transition by norbormide. *Biochim. Biophys. Acta* **1767**, 980-988 (2007).

42. Bernardi, P. *et al*. The mitochondrial permeability transition from in vitro artifact to disease target. *FEBS J.* **273**, 2077-2099 (2006).

43. Rasola, A. & Bernardi, P. The mitochondrial permeability transition pore and its involvement in cell death and in disease pathogenesis. *Apoptosis* **12**, 815-833 (2007).

44. Pletjushkina, O. Y. *et al*. Effect of oxidative stress on dynamics of mitochondrial reticulum. *Biochim. Biophys. Acta* **1757**, 518-524 (2006).

45. Legros, F., Lombes, A., Frachon, P. & Rojo, M. Mitochondrial fusion in human cells is efficient, requires the inner membrane potential, and is mediated by mitofusins. *Mol. Biol. Cell* **13**, 4343-4354 (2002).

46. De Vos, K. J., Allan, V. J., Grierson, A. J. & Sheetz, M. P. Mitochondrial function and actin regulate dynamin-related protein 1-dependent mitochondrial fission. *Curr. Biol.* **15**, 678-683 (2005).

47. Liot, G. *et al*. Complex II inhibition by 3-NP causes mitochondrial fragmentation and neuronal cell death via an NMDA- and ROS-dependent pathway. *Cell Death Differ.* **16**, 899-909 (2009).

48. Benard, G. *et al*. Mitochondrial bioenergetics and structural network organization. *J. Cell. Sci.* **120**, 838-848 (2007).

49. Sauvanet, C., Duvezin-Caubet, S., di Rago, J. P. & Rojo, M. Energetic requirements and bioenergetic modulation of mitochondrial morphology and dynamics. *Semin. Cell Dev. Biol.* **21**, 558-565 (2010).

50. Rossignol, R. *et al*. Energy substrate modulates mitochondrial structure and oxidative capacity in cancer cells. *Cancer Res.* **64**, 985-993 (2004).

51. Westermann, B. Bioenergetic role of mitochondrial fusion and fission. *Biochimica et Biophysica Acta (BBA) - Bioenergetics* **1817**, 1833-1838 (2012).

52. Chen, H., Chomyn, A. & Chan, D. C. Disruption of fusion results in mitochondrial heterogeneity and dysfunction. *J. Biol. Chem.* **280**, 26185-26192 (2005).

53. Chen, H. *et al*. Mitofusins Mfn1 and Mfn2 coordinately regulate mitochondrial fusion and are essential for embryonic development. *J. Cell Biol.* **160**, 189-200 (2003).

54. Scheckhuber, C. Q. *et al*. Reducing mitochondrial fission results in increased life span and fitness of two fungal ageing models. *Nat. Cell Biol.* **9**, 99-105 (2007).

55. Scheckhuber, C. Q., Wanger, R. A., Mignat, C. A. & Osiewacz, H. D. Unopposed mitochondrial fission leads to severe lifespan shortening. *Cell. Cycle* **10**, 3105-3110 (2011).

56. Sato, A., Nakada, K. & Hayashi, J. Mitochondrial dynamics and aging: Mitochondrial interaction preventing individuals from expression of respiratory deficiency caused by mutant mtDNA. *Biochim. Biophys. Acta* **1763**, 473-481 (2006).

57. Tondera, D. *et al*. SLP-2 is required for stress-induced mitochondrial hyperfusion. *EMBO J.* **28**, 1589-1600 (2009).

58. Twig, G., Hyde, B. & Shirihai, O. S. Mitochondrial fusion, fission and autophagy as a quality control axis: the bioenergetic view. *Biochim. Biophys. Acta* **1777**, 1092-1097 (2008).

59. Yu-Wai-Man, P., Bailie, M., Atawan, A., Chinnery, P. F. & Griffiths, P. G. Pattern of retinal ganglion cell loss in dominant optic atrophy due to OPA1 mutations. *Eye* **25**, 596-602 (2011).

60. Yu-Wai-Man, P. *et al*. Genetic screening for OPA1 and OPA3 mutations in patients with suspected inherited optic neuropathies. *Ophthalmology* **118**, 558-563 (2011).

61. Alexander, C. *et al*. OPA1, encoding a dynamin-related GTPase, is mutated in autosomal dominant optic atrophy linked to chromosome 3q28. *Nat. Genet.* **26**, 211-215 (2000).

62. Beumer, K. J. *et al*. Efficient gene targeting in Drosophila by direct embryo injection with zinc-finger nucleases. *Proc. Natl. Acad. Sci. U. S. A.* **105**, 19821-19826 (2008).

63. Wang, A., Fann, M., Yu, H. & Yen, M. OPA1 expression in the human retina and optic nerve. *Exp. Eye Res.* **83**, 1171-1178 (2006).

64. Yu-Wai-Man, P. *et al*. The Prevalence and Natural History of Dominant Optic Atrophy Due to OPA1 Mutations. *Ophthalmology* **117**, 1538-1546.e1 (2010).

65. Marchbank, N. J. *et al*. Deletion of the OPA1 gene in a dominant optic atrophy family: evidence that haploinsufficiency is the cause of disease. *J. Med. Genet.* **39** (2002).

66. Amati-Bonneau, P. *et al*. OPA1 R445H mutation in optic atrophy associated with sensorineural deafness. *Ann. Neurol.* **58**, 958-963 (2005).

67. Leruez, S. *et al*. Sensorineural hearing loss in OPA1-linked disorders. *Brain* **136** (2013).

68. Amati-Bonneau, P. *et al*. OPA1 mutations induce mitochondrial DNA instability and optic atrophy 'plus' phenotypes. *Brain* **131**, 338-351 (2008).

69. Yu-Wai-Man, P. *et al*. Multi-system neurological disease is common in patients with OPA1 mutations. *Brain* **133**, 771-786 (2010).

70. Liskova, P. *et al*. Novel OPA1 missense mutation in a family with optic atrophy and severe widespread neurological disorder. *Acta Ophthalmol.* **91**, e225-e231 (2013).

71. Frezza, C. *et al*. OPA1 Controls Apoptotic Cristae Remodeling Independently from Mitochondrial Fusion. *Cell* **126**, 177-189 (2006).

72. Jackson, G. R. Guide to understanding Drosophila models of neurodegenerative diseases. *PloS Biol.* **6**, 0236-0239 (2008).

73. Cauchi, R. J. & Van Den Heuvel, M. The fly as a model for neurodegenerative diseases: Is it worth the jump? *Neurodegenerative Dis.* **3**, 338-356 (2006).

74. Chan, H. Y. E. & Bonini, N. M. Drosophila models of human neurodegenerative disease. *Cell Death Differ.* **7**, 1075-1080 (2000).

75. Debattisti, V. & Scorrano, L. D. melanogaster, mitochondria and neurodegeneration: Small model organism, big discoveries. *Mol. Cell. Neurosci.* **55**, 77-86 (2013).

76. Dorn II, G. W. *et al*. MARF and Opa1 control mitochondrial and cardiac function in Drosophila. *Circ. Res.* **108**, 12-17 (2011).

77. Tang, S., Le, P. K., Tse, S., Wallace, D. C. & Huang, T. Heterozygous mutation of Opa1 in Drosophila shortens lifespan mediated through increased reactive oxygen species production. *PLoS ONE* **4** (2009).

78. Shahrestani, P. *et al*. Heterozygous mutation of Drosophila Opa1 causes the development of multiple organ abnormalities in an age-dependent and organ-specific manner. *PLoS ONE* **4** (2009).

79. Brachmann, C. B. & Cagan, R. L. Patterning the fly eye: the role of apoptosis. *Trends in Genetics* **19**, 91-96 (2003).

80. Bassett, A. R. & Liu, J. CRISPR/Cas9 and Genome Editing in Drosophila. *Journal of Genetics and Genomics* **41**, 7-19 (2014).

81. Liu, J. *et al*. Efficient and Specific Modifications of the Drosophila Genome by Means of an Easy TALEN Strategy. *Journal of Genetics and Genomics* **39**, 209-215 (2012).

82. Bibikova, M., Golic, M., Golic, K. G. & Carroll, D. Targeted chromosomal cleavage and mutagenesis in Drosophila using zinc-finger nucleases. *Genetics* **161**, 1169-1175 (2002).

83. Bibikova, M., Beumer, K., Trautman, J. K. & Carroll, D. Enhancing gene targeting with designed zinc finger nucleases. *Science* **300**, 764 (2003).

84. Ishino, Y., Shinagawa, H., Makino, K., Amemura, M. & Nakatura, A. Nucleotide sequence of the iap gene, responsible for alkaline phosphatase

isoenzyme conversion in Escherichia coli, and identification of the gene product. *J. Bacteriol.* **169**, 5429-5433 (1987).

85. Jansen, R., Van Embden, J. D. A., Gaastra, W. & Schouls, L. M. Identification of genes that are associated with DNA repeats in prokaryotes. *Mol. Microbiol.* **43**, 1565-1575 (2002).

86. Barrangou, R. *et al*. CRISPR provides acquired resistance against viruses in prokaryotes. *Science* **315**, 1709-1712 (2007).

87. Garneau, J. E. *et al*. The CRISPR/cas bacterial immune system cleaves bacteriophage and plasmid DNA. *Nature* **468**, 67-71 (2010).

88. Gasiunas, G., Barrangou, R., Horvath, P. & Siksnys, V. Cas9-crRNA ribonucleoprotein complex mediates specific DNA cleavage for adaptive immunity in bacteria. *Proc. Natl. Acad. Sci. U. S. A.* **109**, E2579-E2586 (2012).

89. Jinek, M. *et al*. A programmable dual-RNA-guided DNA endonuclease in adaptive bacterial immunity. *Science* **337**, 816-821 (2012).

90. Cong, L. *et al*. Multiplex genome engineering using CRISPR/Cas systems. *Science* **339**, 819-823 (2013).

91. Wang, H. *et al*. One-Step Generation of Mice Carrying Mutations in Multiple Genes by CRISPR/Cas-Mediated Genome Engineering. *Cell* **153**, 910-918 (2013).

92. Bassett, A. R., Tibbit, C., Ponting, C. P. & Liu, J. -. Mutagenesis and homologous recombination in Drosophila cell lines using CRISPR/Cas9. *Biol. Open* **3**, 42-49 (2014).

93. Yu, Z. *et al*. Highly efficient genome modifications mediated by CRISPR/Cas9 in Drosophila. *Genetics* **195**, 289-291 (2013).

94. Shan, Q. *et al*. Targeted genome modification of crop plants using a CRISPR-Cas system. *Nat. Biotechnol.* **31**, 686-688 (2013).

95. Dicarlo, J. E. *et al*. Genome engineering in Saccharomyces cerevisiae using CRISPR-Cas systems. *Nucleic Acids Res.* **41**, 4336-4343 (2013).

96. Gratz, S. J. *et al*. Genome engineering of Drosophila with the CRISPR RNA-guided Cas9 nuclease. *Genetics* **194**, 1029-1035 (2013).

97. Mali, P. *et al*. RNA-guided human genome engineering via Cas9. *Science* **339**, 823-826 (2013).

98. Esvelt, K. M. *et al*. Orthogonal Cas9 proteins for RNA-guided gene regulation and editing. *Nat. Methods* **10**, 1116-1123 (2013).

99. Mojica, F. J. M., Díez-Villaseñor, C., García-Martínez, J. & Almendros, C. Short motif sequences determine the targets of the prokaryotic CRISPR defence system. *Microbiology* **155**, 733-740 (2009).

100. Bassett, A., Tibbit, C., Ponting, C. & Liu, J. Highly Efficient Targeted Mutagenesis of Drosophila with the CRISPR/Cas9 System. *Cell Reports* **4**, 220-228 (2013).

101. Gratz, S. J., Wildonger, J., Harrison, M. M. & O'Connor-Giles, K. M. CRISPR/Cas9-mediated genome engineering and the promise of designer flies on demand. *Fly* **7** (2013).

102. Sebo, Z. L., Lee, H. B., Peng, Y. & Guo, Y. A simplified and efficient germline-specific CRISPR/Cas9 system for Drosophila genomic engineering. *Fly* **8** (2014).

103. Kondo, S. & Ueda, R. Highly Improved gene targeting by germline-specific Cas9 expression in Drosophila. *Genetics* **195**, 715-721 (2013).

104. Ren, X. *et al*. Optimized gene editing technology for Drosophila melanogaster using germ line-specific Cas9. *Proc. Natl. Acad. Sci. U. S. A.* **110**, 19012-19017 (2013).

105. Smih, F., Rouet, P., Romanienko, P. J. & Jasin, M. Double-strand breaks at the target locus stimulate gene targeting in embryonic stem cells. *Nucleic Acids Res.* **23**, 5012-5019 (1995).

106. Rong, Y. S. & Golic, K. G. Gene targeting by homologous recombination in Drosophila. *Science* **288**, 2013-2018 (2000).

107. Beumer, K. J., Trautman, J. K., Mukherjee, K. & Carroll, D. Donor DNA utilization during gene targeting with zinc-finger nucleases. *G3 Genes Genome Genet.* **3**, 657-664 (2013).

108. Yang, H., Wang, H. & Jaenisch, R. Generating genetically modified mice using CRISPR/Cas-mediated genome engineering. *Nat. Protoc.* **9**, 1956-1968 (2014).

109. Trounce, I. A., Kim, Y. L., Jun, A. S. & Wallace, D. C. [42] Assessment of mitochondrial oxidative phosphorylation in patient muscle biopsies, lymphoblasts, and transmitochondrial cell lines. *Methods Enzymol.* **264**, 484-509 (1996).

110. Hudson, G. *et al*. Mutation of OPA1 causes dominant optic atrophy with external ophthalmoplegia, ataxia, deafness and multiple mitochondrial DNA deletions: A novel disorder of mtDNA maintenance. *Brain* **131**, 329-337 (2008).

111. Zanna, C. *et al*. OPA1 mutations associated with dominant optic atrophy impair oxidative phosphorylation and mitochondrial fusion. *Brain* **131**, 352-367 (2008).